Supramolecular Chemistry and Molecular Self-Assembly

M2 – Ecole polytechnique - Université Paris-Saclay
France

Grids, Catenanes, Rotaxanes *and* *Molecular engines*

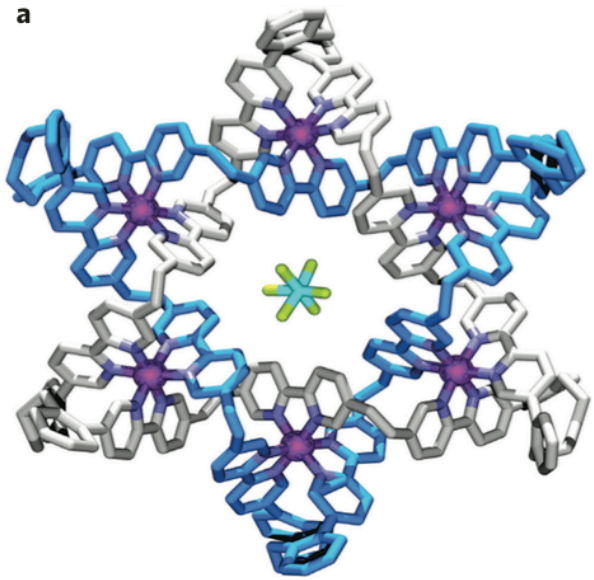

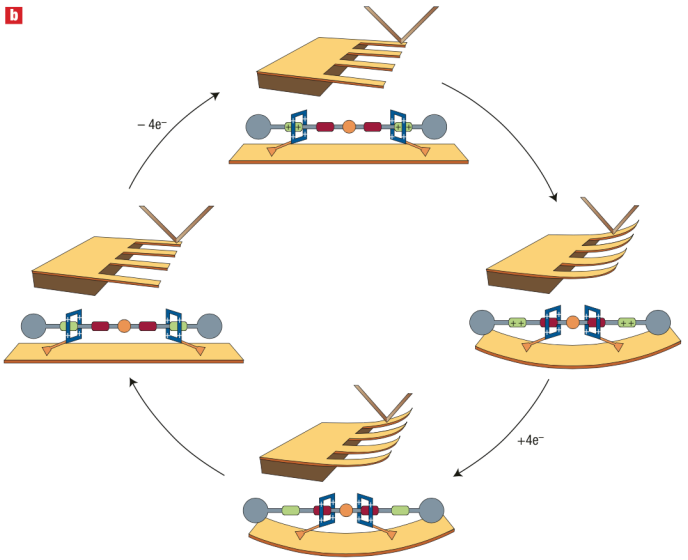

Molecular Grids: the beginning

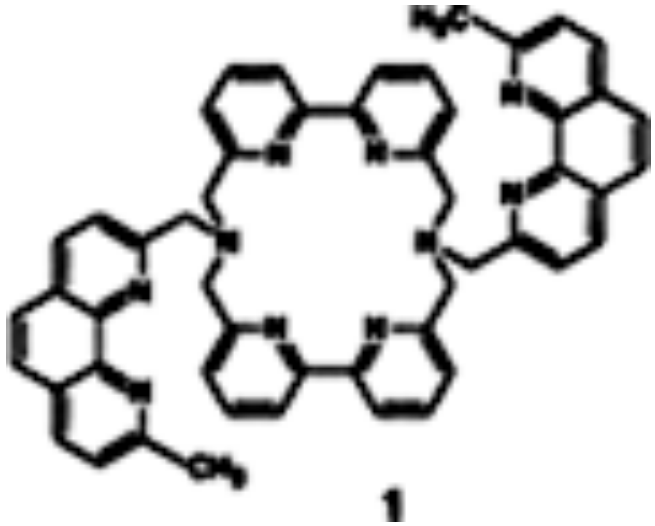

1

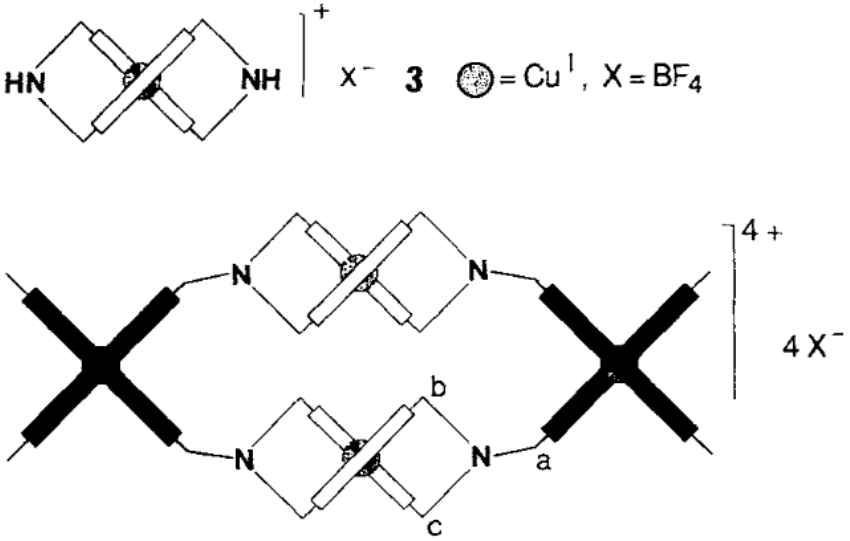

4 ⊙ = Cu^{I}, X = ClO_4, BF_4

5 ⊙ = Ag^{I}, X = CF_3SO_3

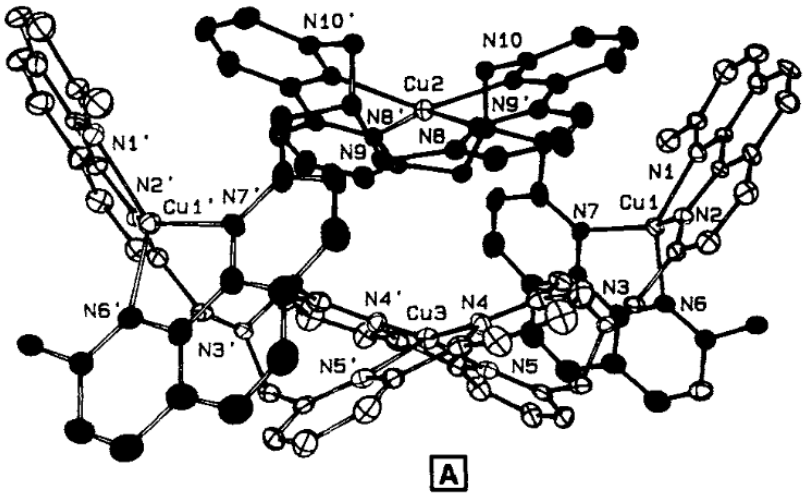

Ziessel, *Angew. Chem., Int. Ed.* **1993,** *32*, 877.

Molecular Grids: (2 x 2) grids

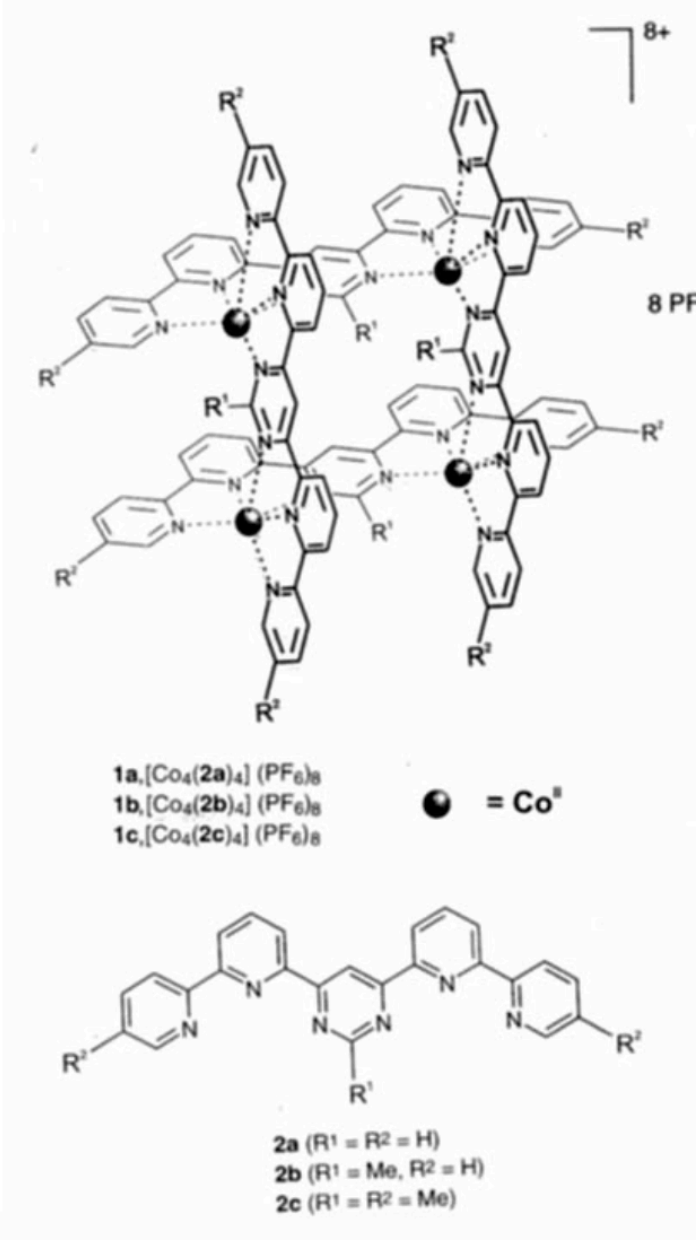

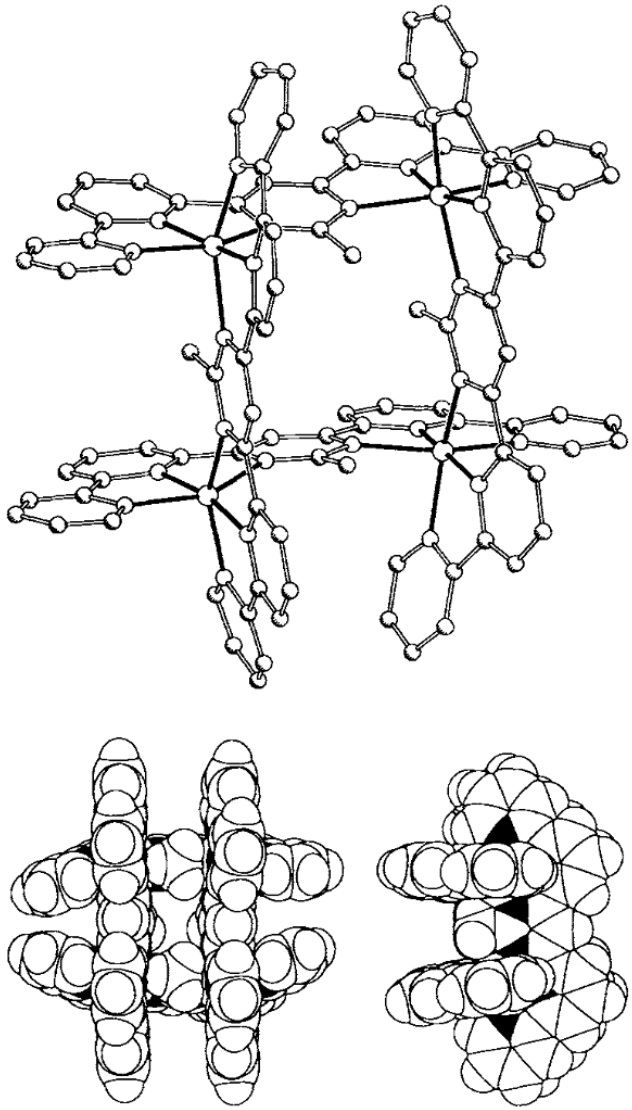

Lehn, *Angew. Chem., Int. Ed.* **1997,** *36*, 1842.

Molecular Grids: (3 x 3) grids

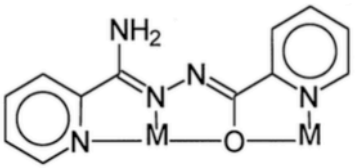

poap

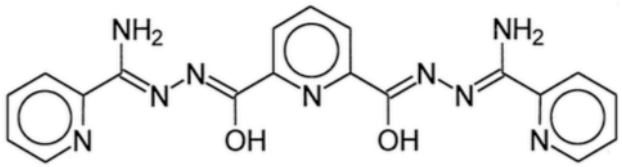

2poap

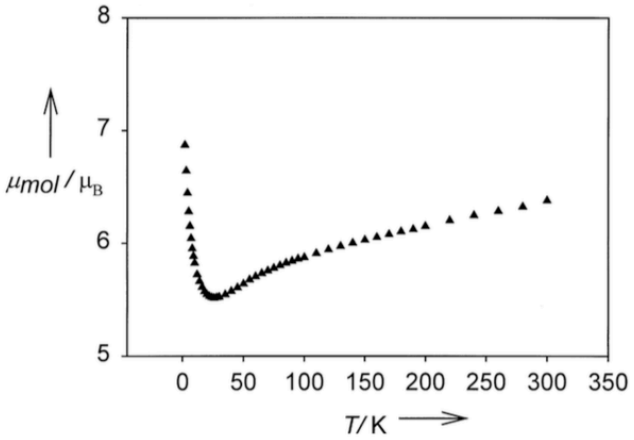

Figure 3. Variable-temperature magnetism for **2** plotted as magnetic moment (μ_B) per mole versus temperature (0.1 T field).

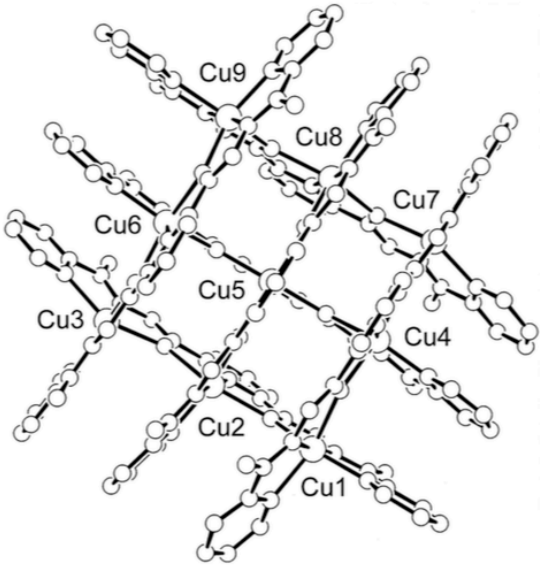

Figure 1. Structural representation of the cation $[Cu_9(2poap\text{-}H)_6]^{12+}$ in **2** (hydrogen atoms omitted for clarity). Selected bond lengths [Å] and angles [°]: Cu5-N14 1.941(10), Cu5-N41 1.912(11), Cu5-O3 2.163(7), Cu5-O4 2.197(7), Cu5-O9 2.210(10), Cu5-O10 2.199(9), Cu1-Cu2 4.148(8), Cu2-Cu3 4.198(7), Cu3-Cu6 4.169(8), Cu6-Cu9 4.085(9), Cu9-Cu8 4.2187, Cu8-Cu7 4.106(7), Cu7-Cu4 4.116(8), Cu4-Cu1 4.227(8), Cu2-Cu5 4.069(7), Cu6-Cu5 4.048(8), Cu8-Cu5 4.065(8), Cu4-Cu5 4.032(6); Cu-O-Cu 136.5 – 143.6.

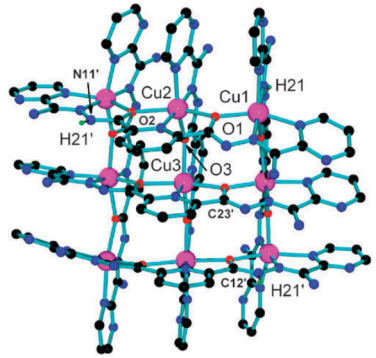

Fig. 16 Structural representation of the cation in $[Cu(II)_9(HL23j^-)_4(L23j^{2-})_2](ClO_4)_{10}$ (**15**).

Thompson, *Angew. Chem., Int. Ed.* **2000** *39*, 3114.

Molecular Grids: (4 x 4) grids

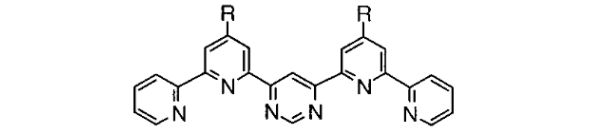

1a R=H

1b

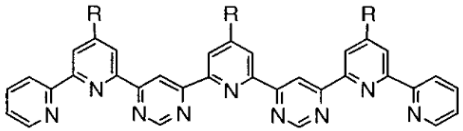

1c

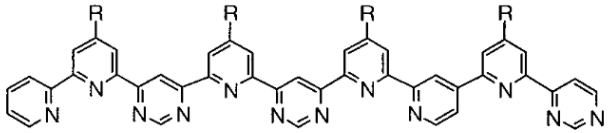

1d

1b, **1c**, **1d** R=$SCH_2CH_2CH_3$

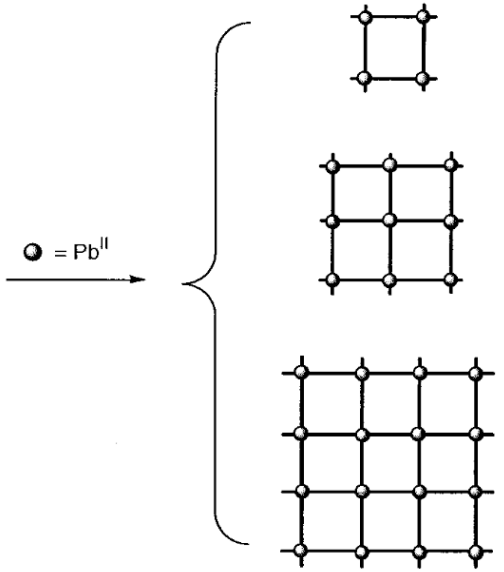

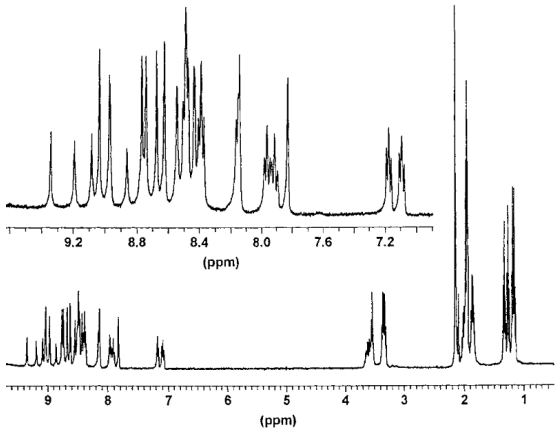

Figure 4. 400 MHz ^{1}H NMR spectrum of a CD_3CN solution of the hexadecanuclear grid-type complex **4** as obtained by self-assembly from ligand **1d** and lead(II) triflate; for signal assignment, see Experimental Section.

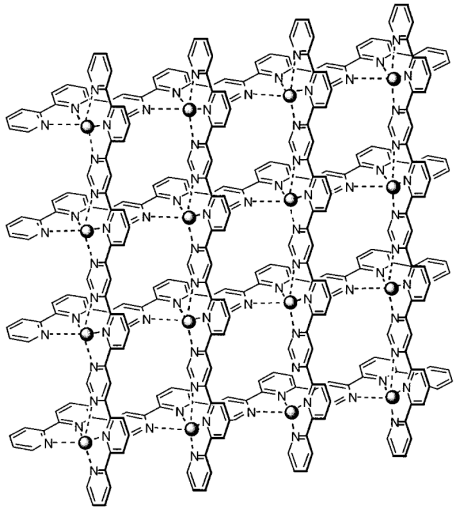

4 (ligand **1d**, R omitted)

Lehn, *Chem. Eur. J.* **1999** *5*, 1803.

Molecular Grids: (5 x 5) grids

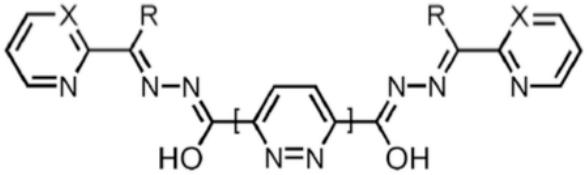

H_2L26a (X=CH,R=NH_2), H_2L26b (X=CH,R=H), H_2L26c (X=N,R=NH_2)

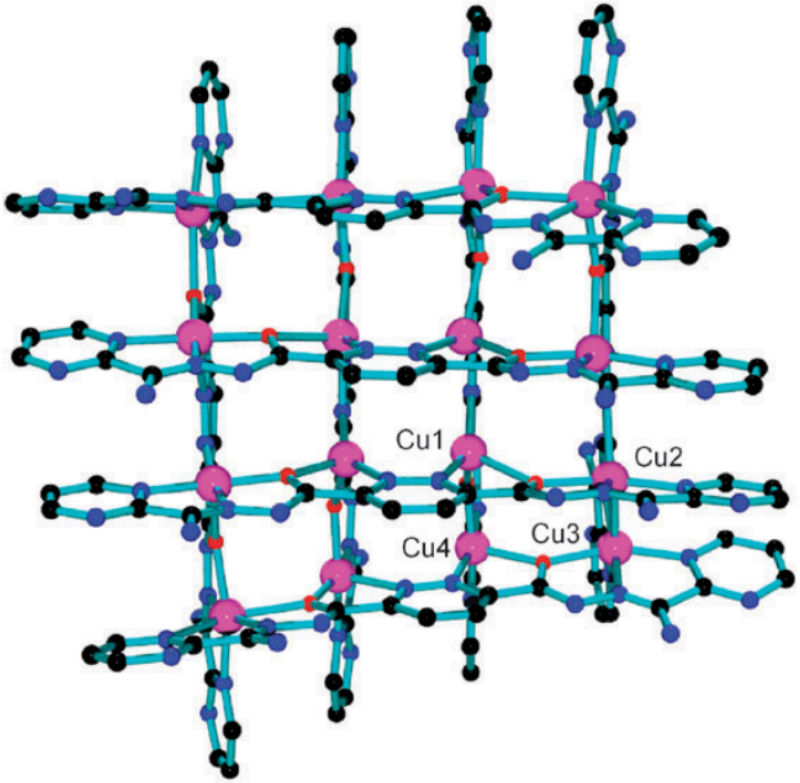

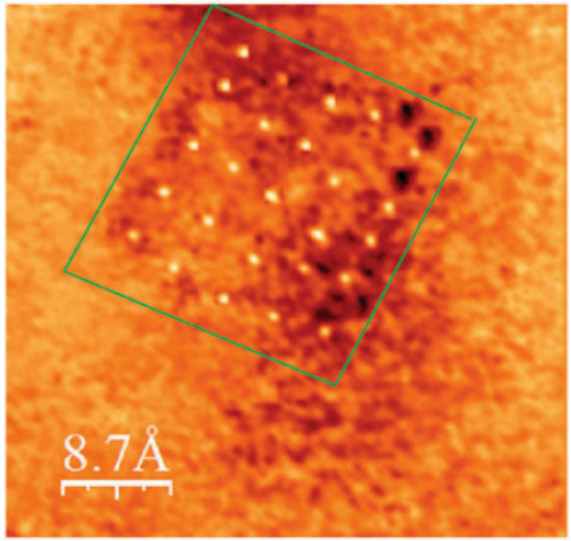

Fig. 25 CITS image of [Mn_{25}] [5 × 5] grid core on HOPG.

Thompson, *Chem. Soc. Rev.* **2009** *38*, 2334.

Molecular Grids: Self assemblies and mixtures

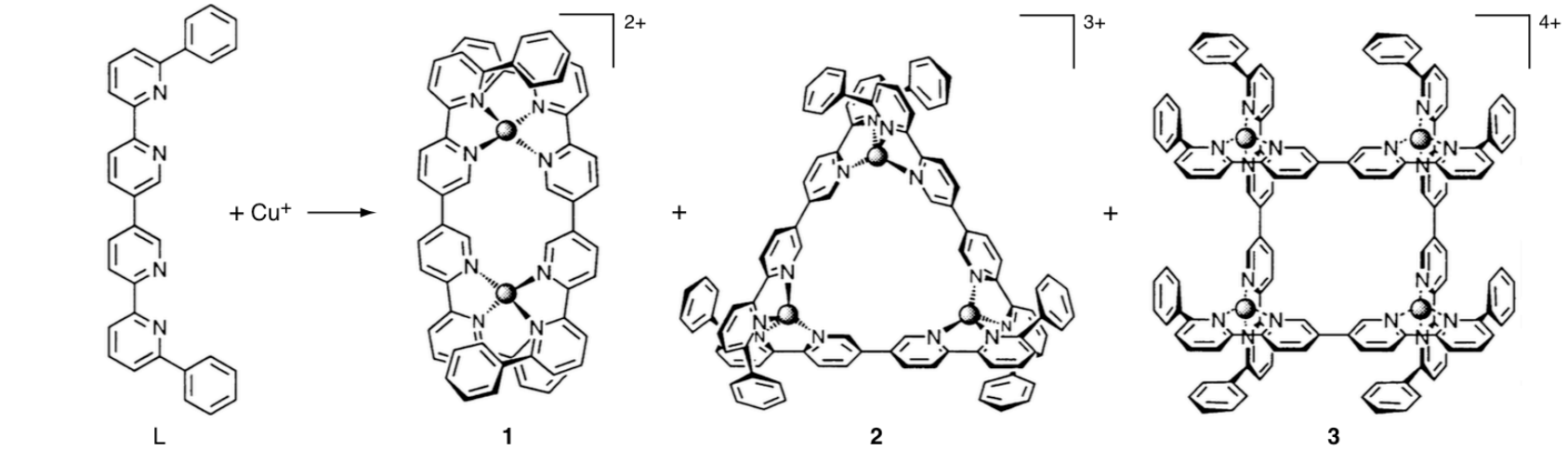

Scheme 1 Self-assembly of an equilibrating mixture of the double-helical **1**, triangular **2** and square [2 × 2] grid **3** complexes from L and Cu^{I}. Complexes **2** and **3** can in principle exist in different interwoven structures; only one structure is shown here.

Lehn, *Chem. Commun.* **1997**, 1323.

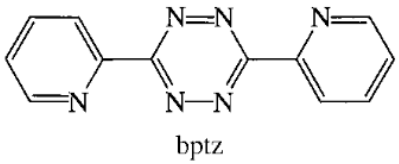

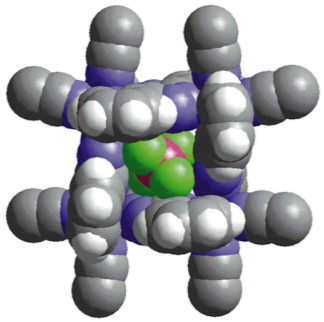

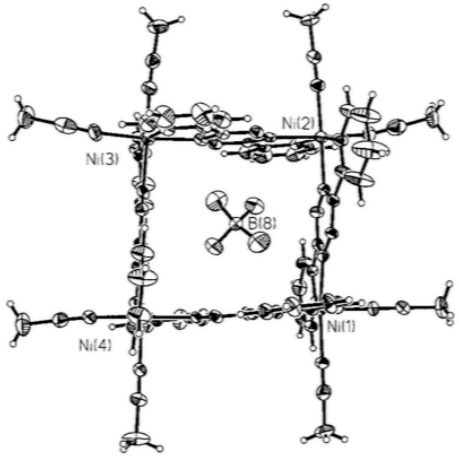

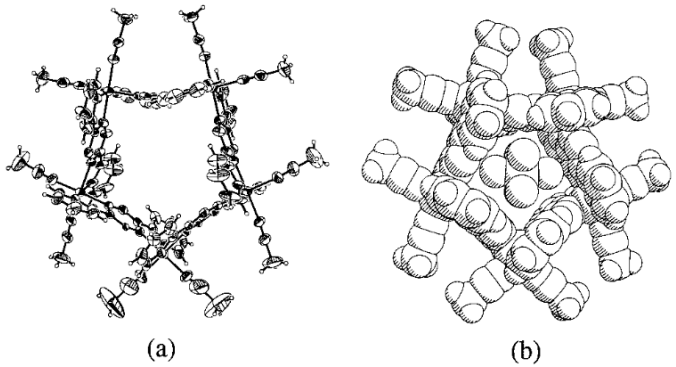

Figure 2. (a) ORTEP drawing of the molecular structure of the $[\mathbf{1}]^{10+}$ ion. Thermal ellipsoids are drawn at the 50% probability level and (b) space-filling diagram of the molecular cation with the encapsulated $[SbF_6]^-$ ion.

Dunbar, *Angew. Chem. Int. Ed.* **1999**, 3477, *J. Am. Chem. Soc.*, **2001**, *123,* 773

Molecular Grids: Magnetism

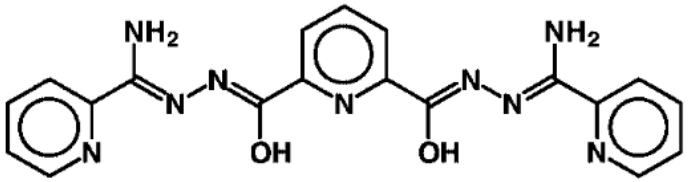

2poapH2

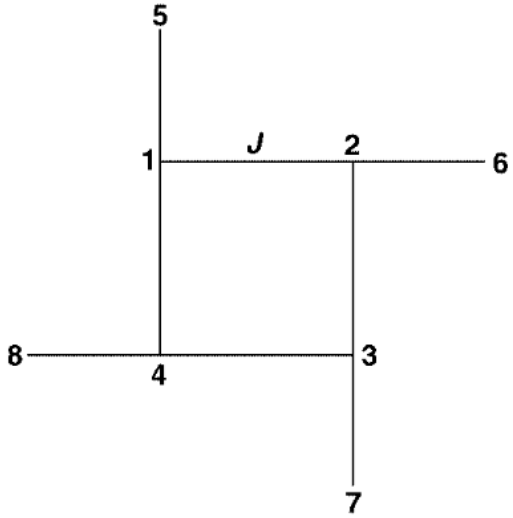

Scheme 1

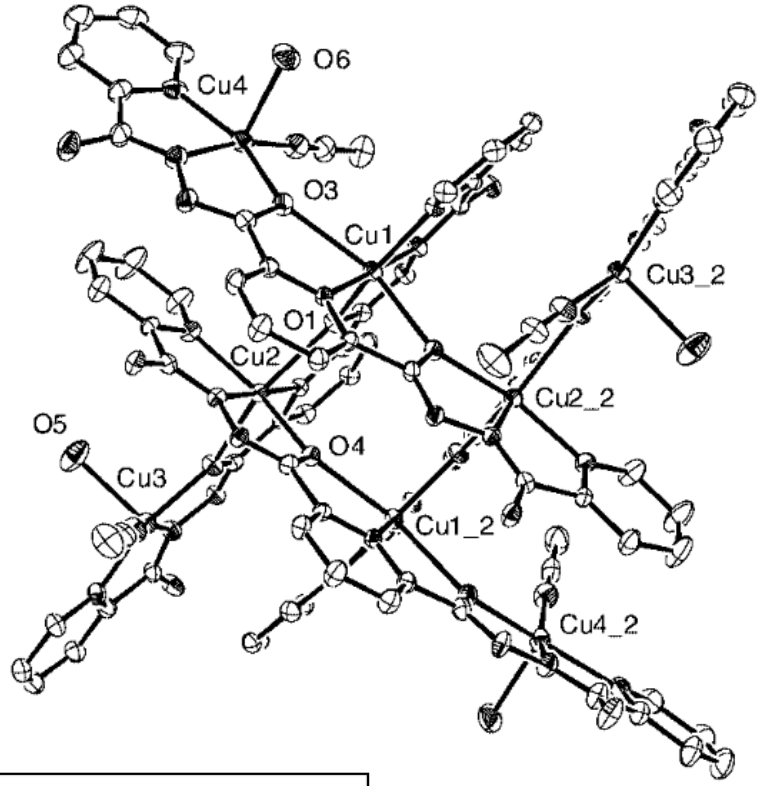

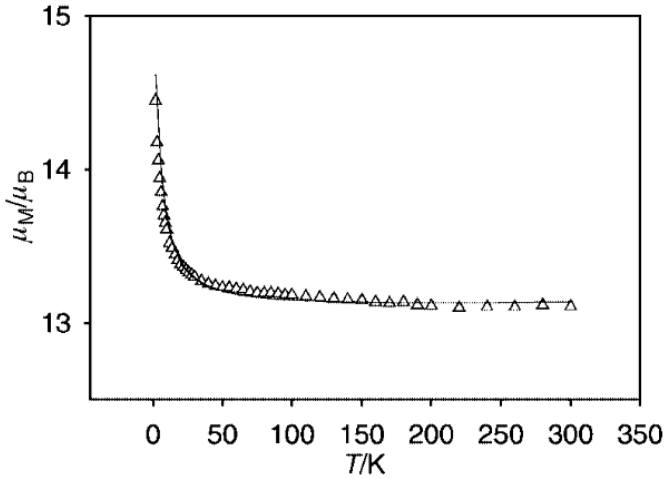

Thompson, *Chem. Commun.*, **2001**, 1170–1171

$$H = 2J(S1S2 + S2S3 + S3S4 + S1S4 + S1S5 + S2S6 + S3S7 + S4S8)$$

Molecular Grids: Spin States

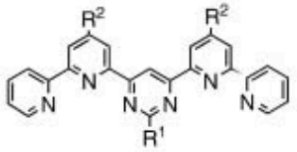

A	$R^1 = H$	$R^2 = H$
B	$R^1 = H$	$R^2 = S^nPr$
C	$R^1 = OH$	$R^2 = H$
D	$R^1 = Me$	$R^2 = H$
E	$R^1 = Ph$	$R^2 = H$
F	$R^1 = p\text{-}Ph\text{-}NMe_2$	$R^2 = H$
G	$R^1 = Ph$	$R^2 = S^nPr$

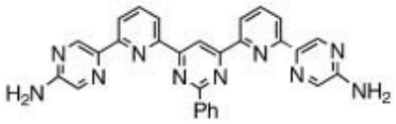

H

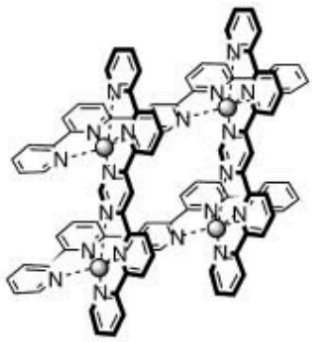

	cation	anion	
	●	X	
1	Fe^{II}	PF_6	L = **A**
2	Fe^{II}	PF_6	L = **B**
3	Fe^{II}	BF_4	L = **C**
4	Fe^{II}	ClO_4	L = **D**
5	Fe^{II}	ClO_4	L = **E**
6	Fe^{II}	ClO_4	L = **F**
7	Fe^{II}	ClO_4	L = **G**
8	Fe^{II}	BF_4	L = **H**

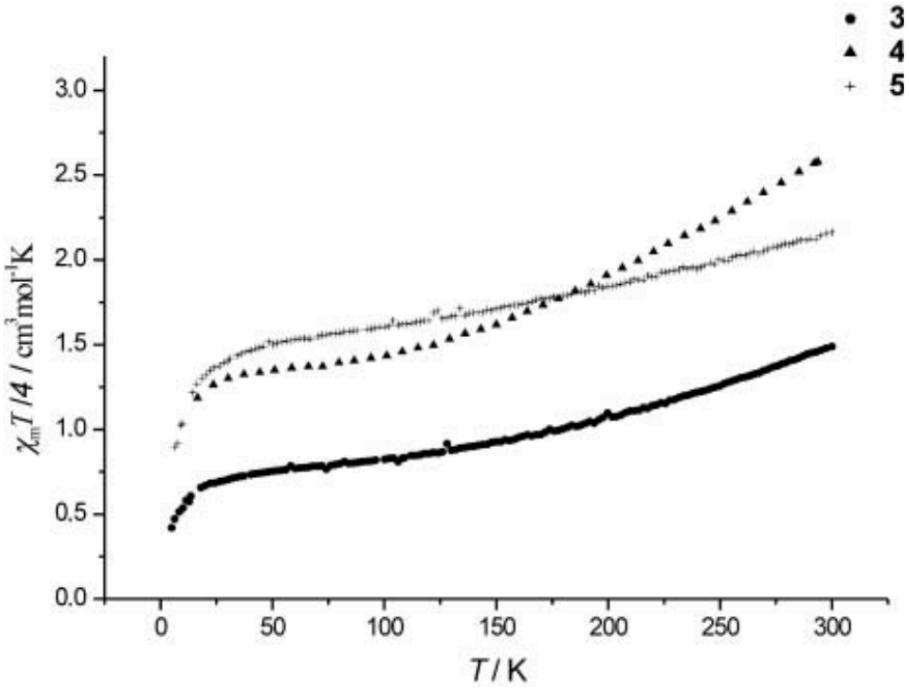

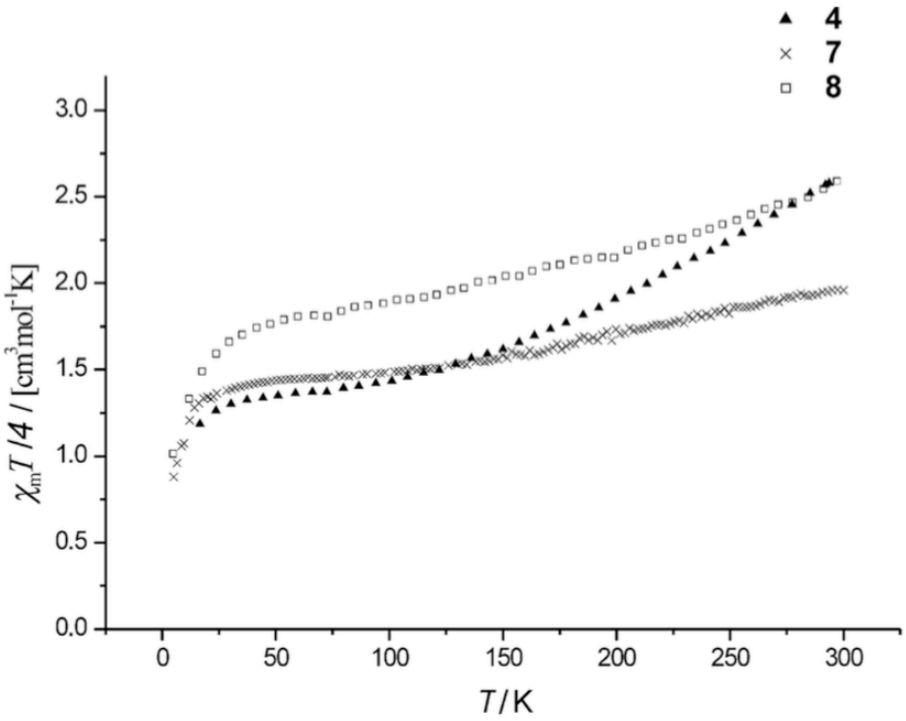

M. Ruben, E. Breuning, J.-M. Lehn, V. Ksenofontov, F. Renz, P. Gütlich, G. Vaughan, *Chem. Eur. J.* **2003**, 9, 4422

Molecular Grids: Redox

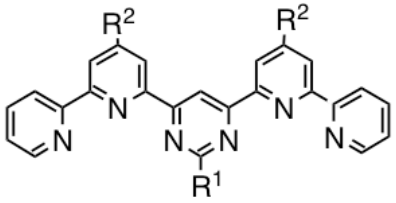

A	R^1 = H	R^2= H
B	R^1 = Ph	R^2= H
C	R^1 = H	R^2=COOMe
D	R^1 = Ph	R^2=COOMe
E	R^1 = Ph	R^2=S*n*Pr

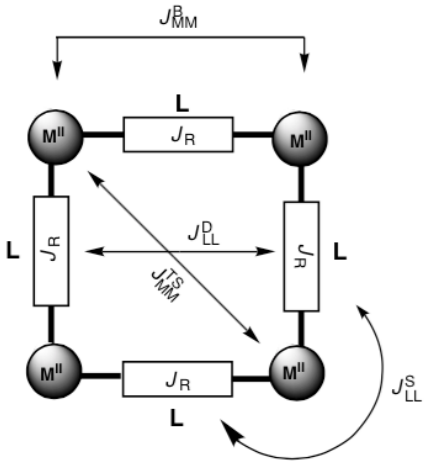

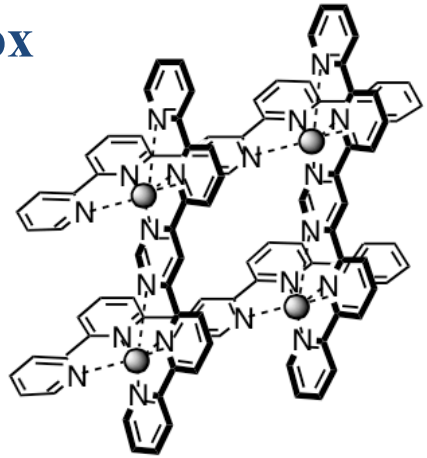

	cation	anion	
	●	X	
1	Co^{II}	BF_4	L = **A**
2	Co^{II}	BF_4	L = **B**
3	Co^{II}	BF_4	L = **C**
4	Co^{II}	BF_4	L = **D**
5	Co^{II}	BF_4	L = **E**
6	Fe^{II}	BF_4	L = **B**
7	Zn^{II}	CF_3SO_3	L = **B**
8	Mn^{II}	ClO_4	L = **B**

C-4

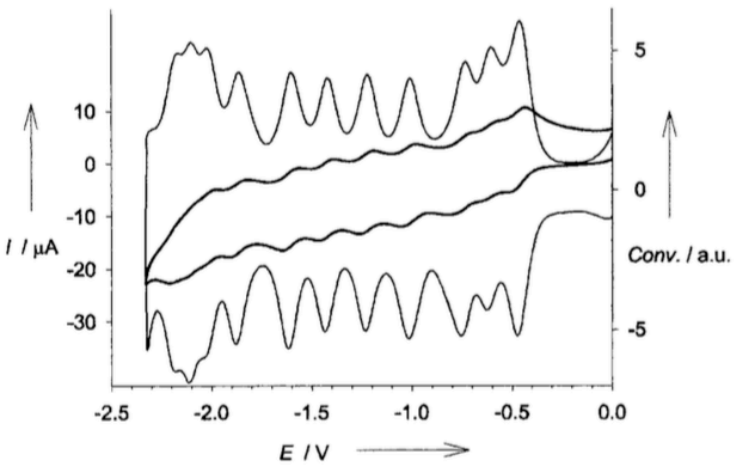

D-4

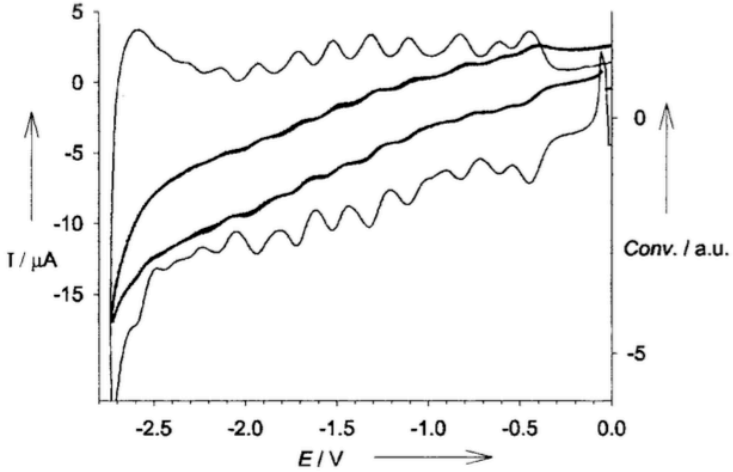

M. Ruben, E. Breuning, M. Barboiu, J.-P. Gisselbrecht, J.-M. Lehn, *Chem. Eur. J.* **2003**, *9*, 291

Molecular Grids: Optical properties

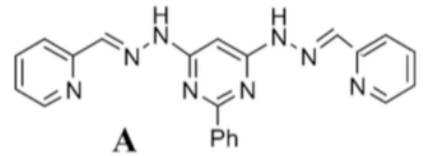

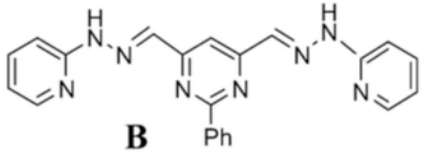

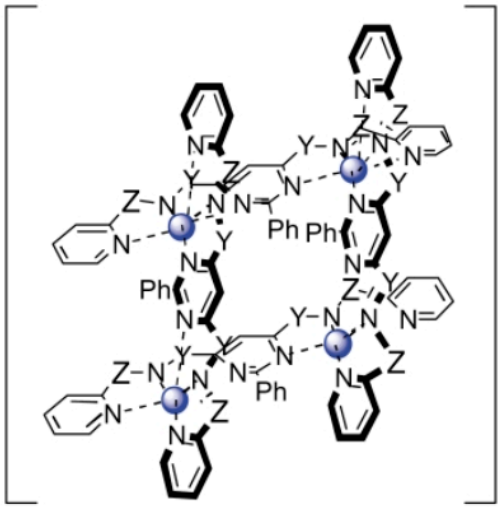

		cation	anion
		●	X
1	$[Co^{II}_4\mathbf{A}_4](BF_4)_8$	Co^{II}	BF_4^-
2	$[Co^{II}_4\mathbf{B}_4](BF_4)_8$	Co^{II}	BF_4^-
3	$[Mn^{II}_4\mathbf{A}_4](ClO_4)_8$	Mn^{II}	ClO_4^-

A -Y-N-Z- = -NH-N=CH-
B -Y-N-Z- = -CH=N-NH-

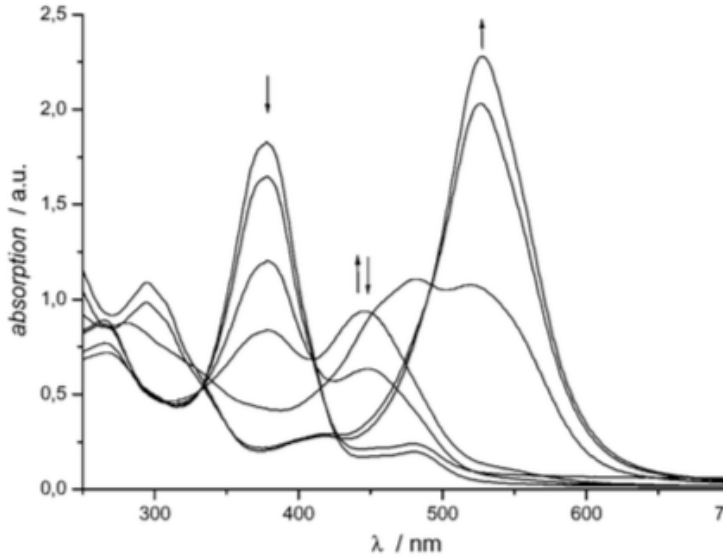

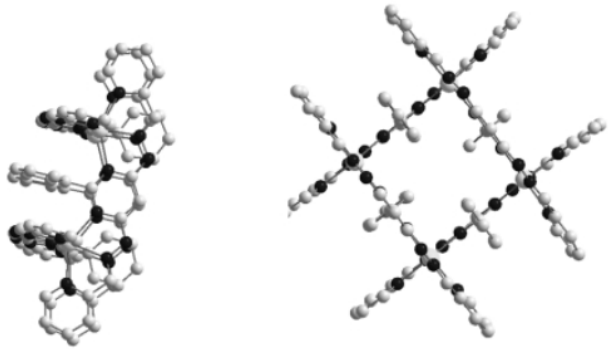

Fig. 3 Colour change of $[Co^{II}_4\mathbf{A}_4](BF_4)_8$ **1** at different pH.

Lehn, *Chem. Commun.*, **2003**, 1338

Rotaxanes and Catenanes

Interlocking of Molecular Threads

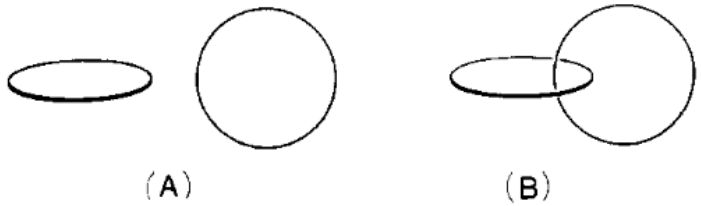

Figure 1.

(2)-Catenane

B is a topological isomers of A and B

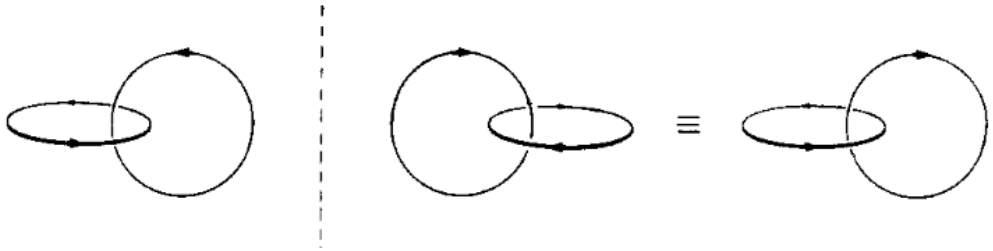

If the rings are directed, chiral catenanes

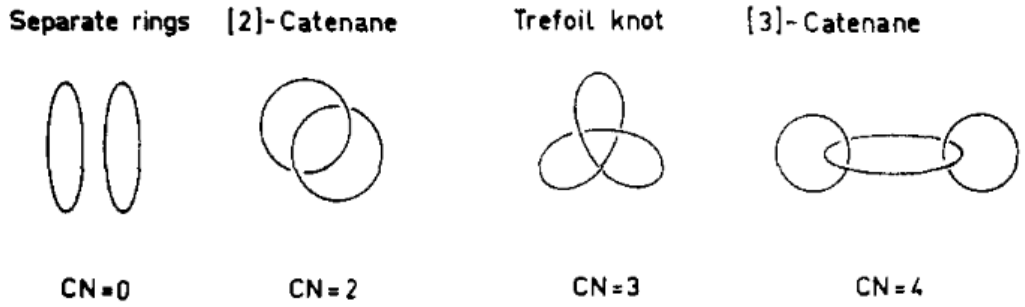

Figure 6. Increasing topological complexity of molecular graphs as defined by their *crossing number* (CN).

Sauvage, *Chem. Rev.*, **1987**

Rotaxanes and Catenanes

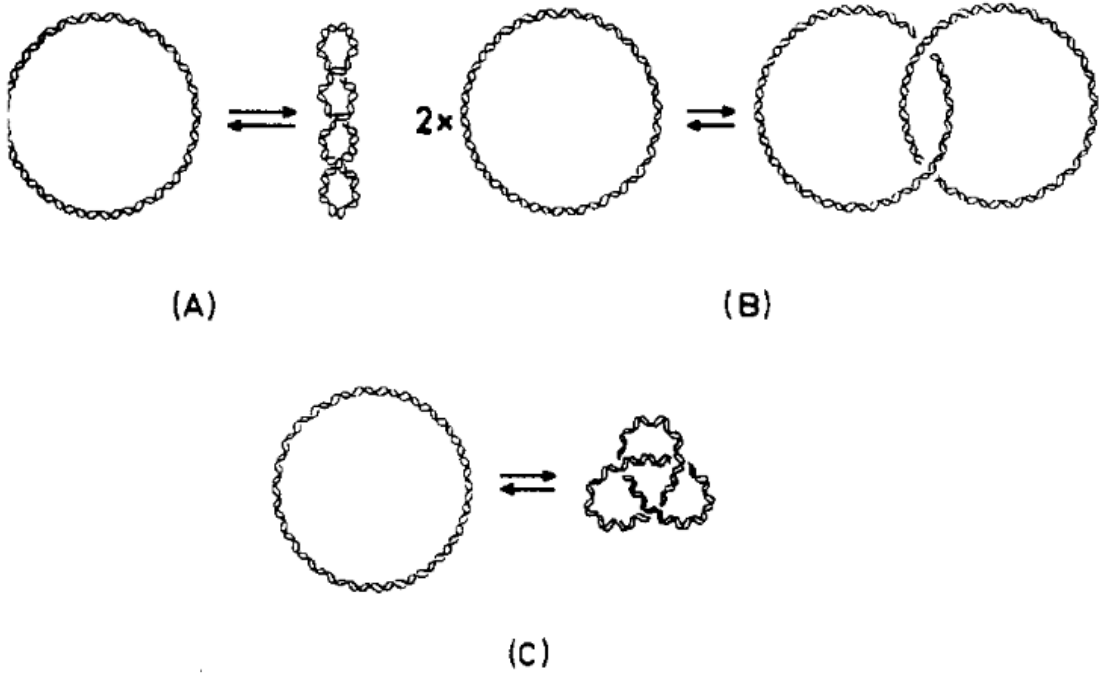

Figure 4. Duplex circular DNA: (A) supercoiled or supertwisted;[17a] (B) catenated or interlocked;[17b] (C) knotted.

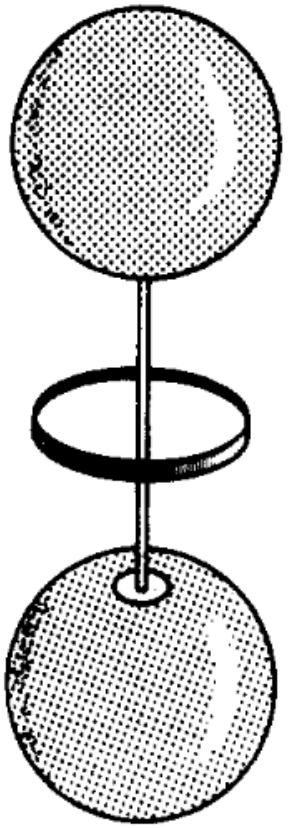

ROTAXANE

In other words, the beauty of some molecules might be independent of shape and rest only in its topological properties. We find this especially true for interlocked rings and knots.

Sauvage, *Chem. Rev.*, **1987**

Catenanes: synthesis

Synthesis of Catenanes by Statistical Threading

A molecular thread A-B, functionalized on both ends, may enter into a macrocycle of adequate size: subsequent cyclization of A-B leads necessarily to two interlocked rings. But since the probability that cyclization occurs while the linear molecule a A-B is threaded through the macrocycle is very small, one can only expect poor yields in this kind of synthesis.

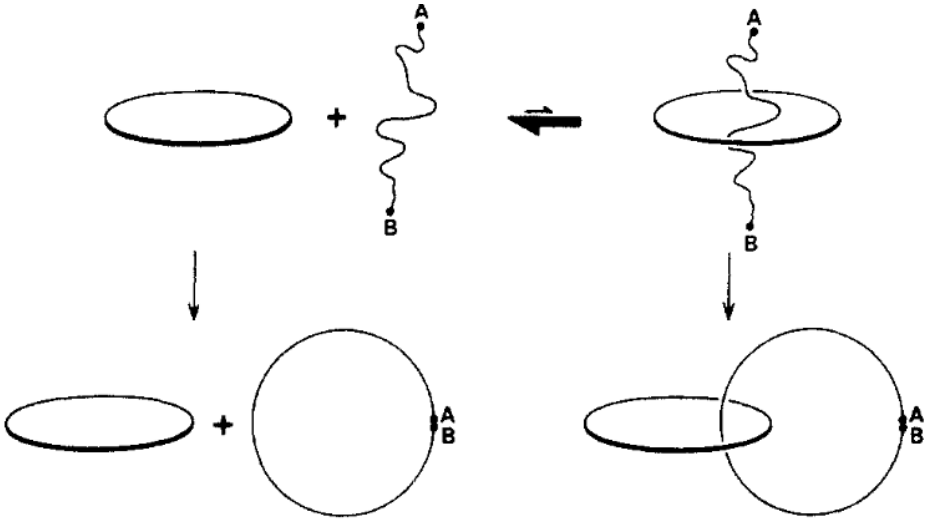

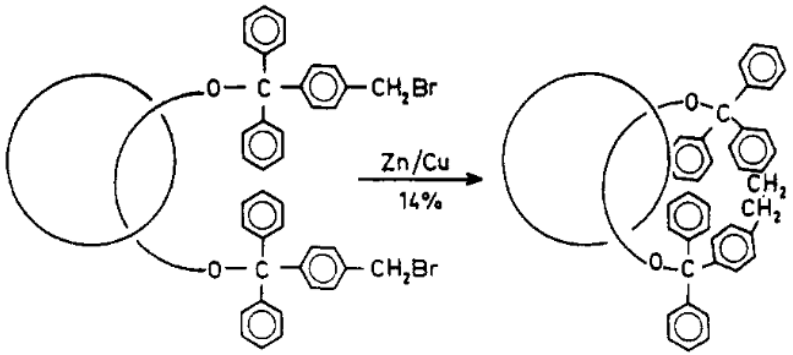

5 6

Agam,G.; Graiver,D.; Zilkha,A. *J.Am.Chem.*Soc.**1976**, *98,* 5206.

The rotaxane **5,** obtained with 18.5% yield by statistical threading of a "crown" polyether by poly(ethy1ene glycol) 400, leads to the catenane **6** after cyclization in high-dilution conditions (14% yield).

Sauvage, *Chem. Rev.*, **1987**

Catenanes: synthesis

Möbius Strip Approach

This approach, already considered by Wasserman and Schill is based on a ladder-shaped molecule in which the ends are able to twist prior to bimacrocyclization.

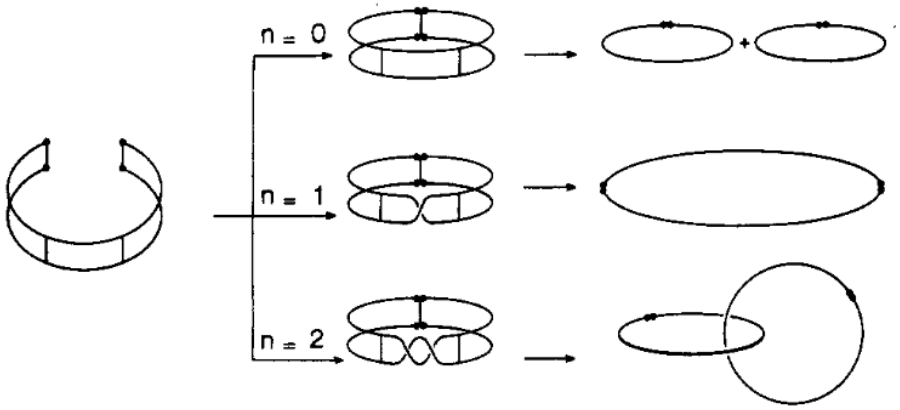

Figure 12. Principle of a catenane synthesis by preliminary construction of a Möbius strip.

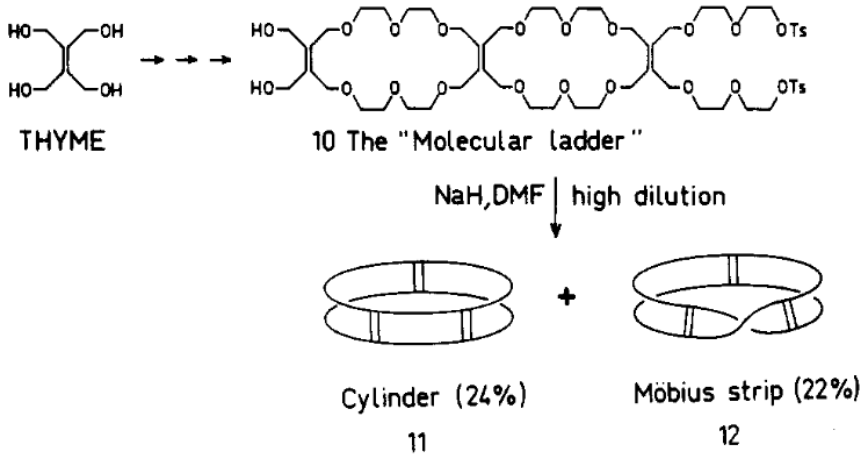

Walba, D. M.; Richards, R. M.; Haltiwanger, R. C. *J. Am. Chem. Soc.* **1982,** 104, 3219.

The statistical probability that the ends of a molecular ladder twist twice before cyclization, leading thus to the required single- full-twisted Mobius strip, remains quite small.

Catenanes: synthesis

Schill-Lüttringhaus Synthesis Directed Catenane (1964)

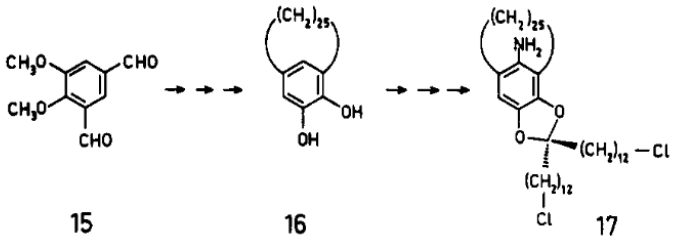

15 16 17

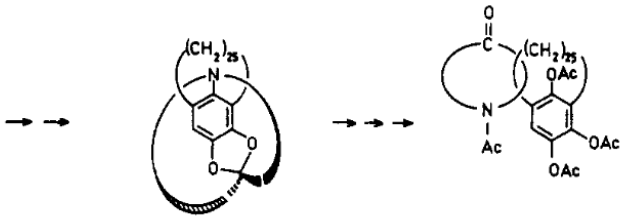

Triansa compound 18 [2]-Catenate 19

Schill, G.; Zollenkopf, H. *Liebigs Ann. Chem.* **1969,** 721, 53

Schill, G.; Luttringhaus, A. *Angew. Chem.* **1964,** 76, 567.

Whatever the precursor used, **17** or **22**, the pathways followed in the above-described syntheses ensure the formation of interlocked rings. Nevertheless, because of the numerous steps involved, large-scale preparation of catenanes via the Schill-Luttringhaus strategy remains a highly difficult task.

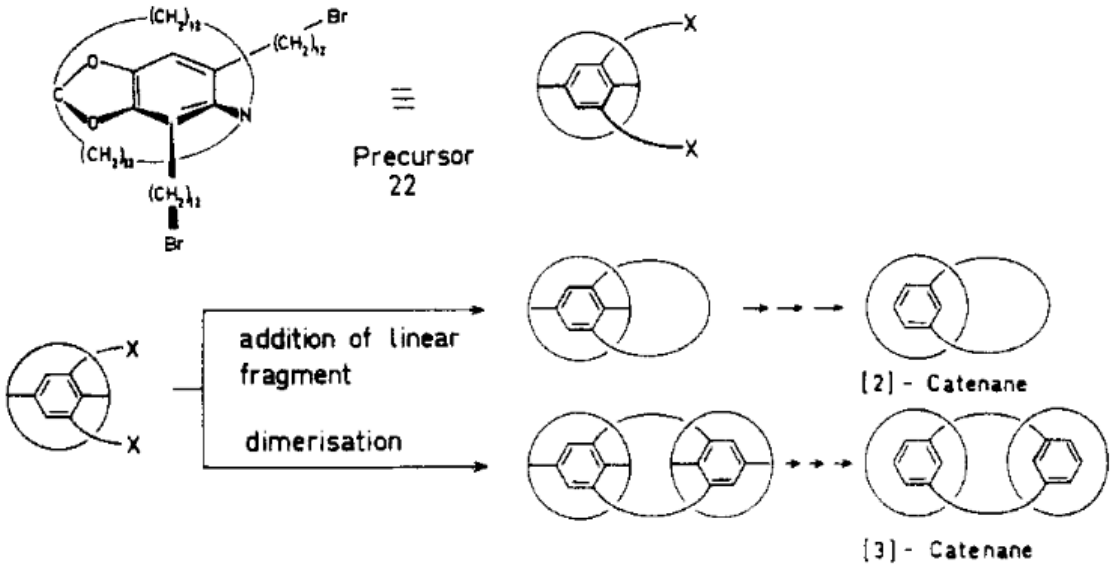

Catenanes: synthesis

Template Synthesis

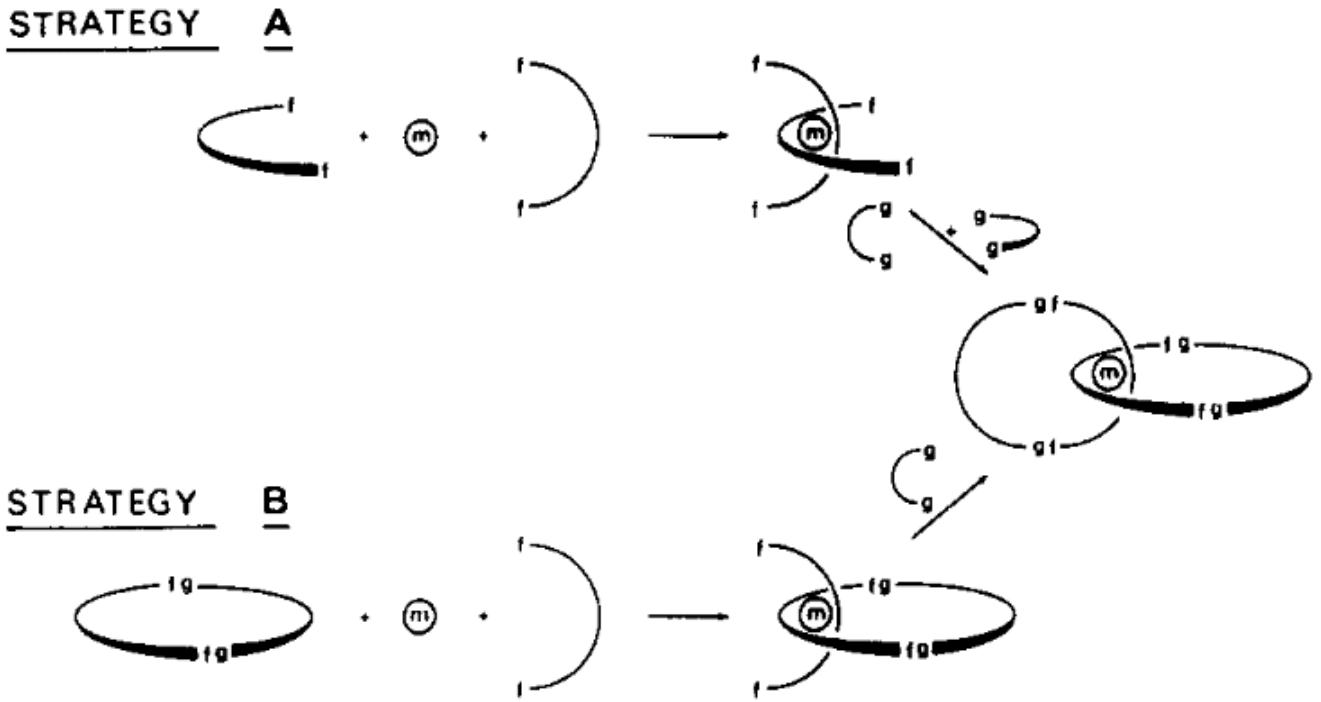

Figure 22. *Synthetic strategies based on a three-dimensional template effect induced by a transition metal.* Functions f and g react to form the links. The molecular fragment f–f interacts with a transition metal (m) bearing or not bearing auxiliary ligands. This metal disposes fragments f–f (linear or already included in a cycle) perpendicular to one another.

Sauvage, *Chem. Rev.*, **1987**

Catenanes: synthesis

Template Synthesis

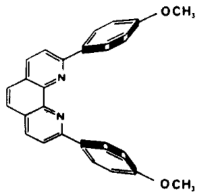

27

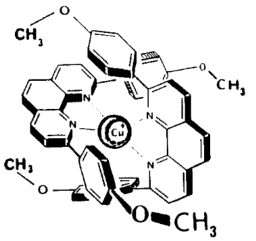

28^+

Figure 25. In the copper(I) complex 28^+, the two highly rigid coordinating subunits **27** fit together while encaging the metal atom.

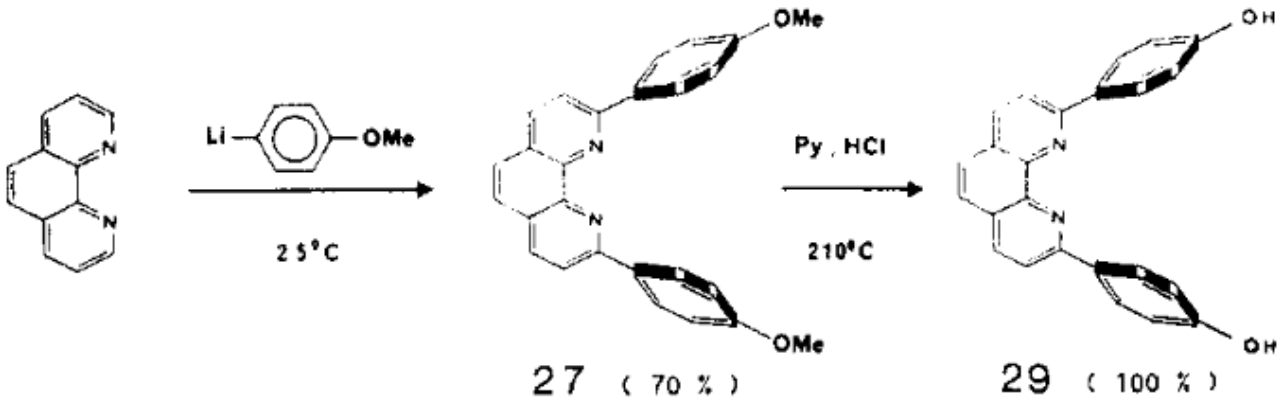

27 (70 %)

29 (100 %)

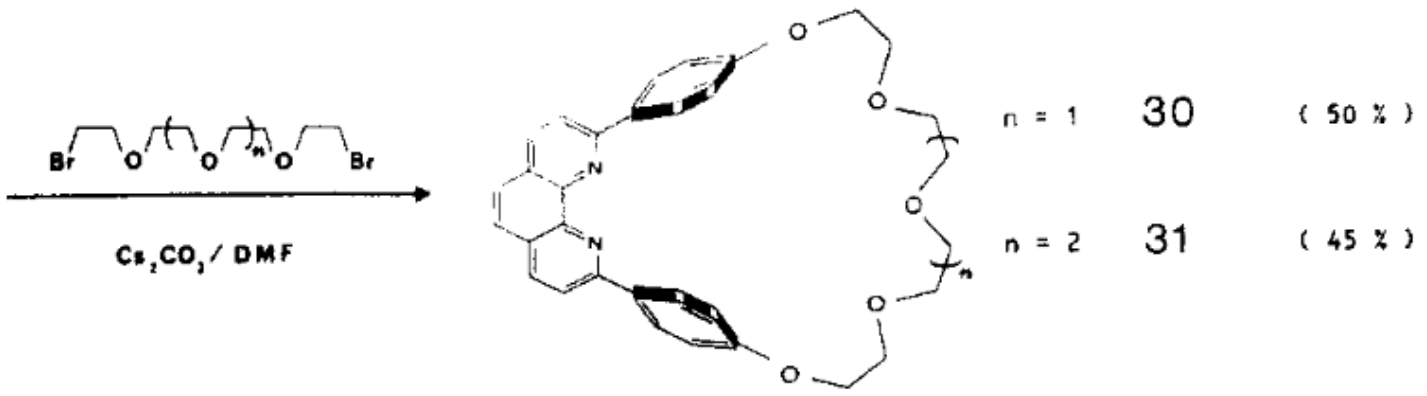

n = 1 **30** (50 %)

n = 2 **31** (45 %)

Catenanes: synthesis

Template Synthesis

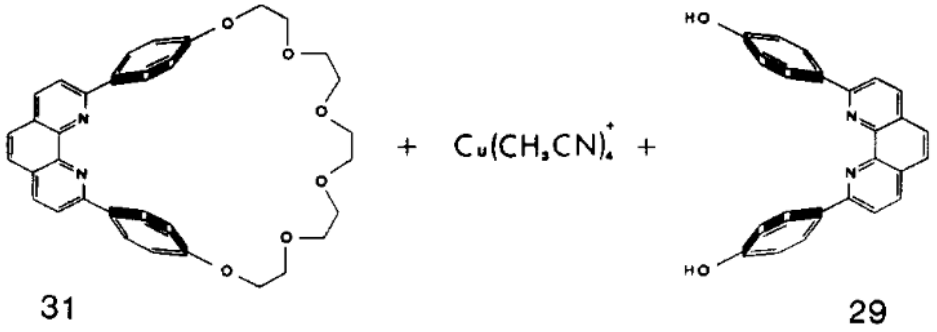

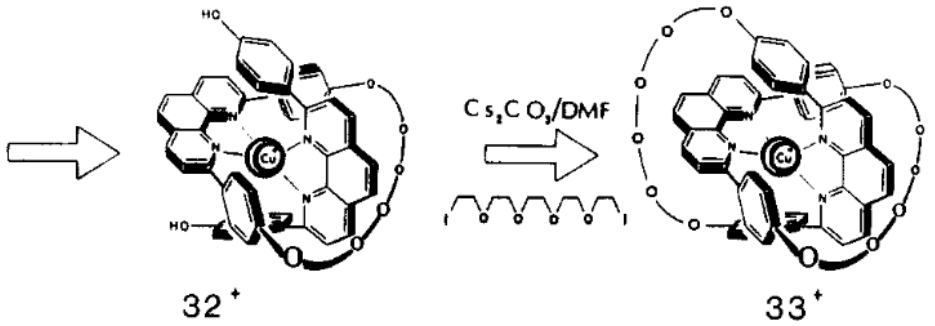

Strategy A

Strategy B

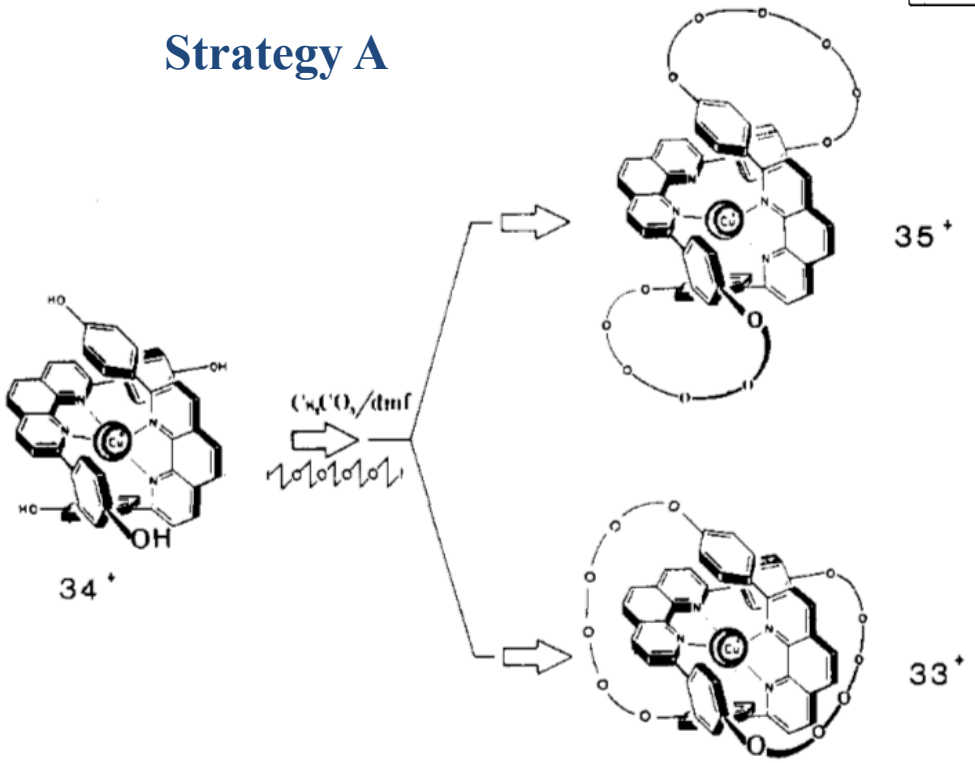

Figure 28. One-pot template synthesis of 33^+ (strategy A).

Catenanes: synthesis

Template Synthesis

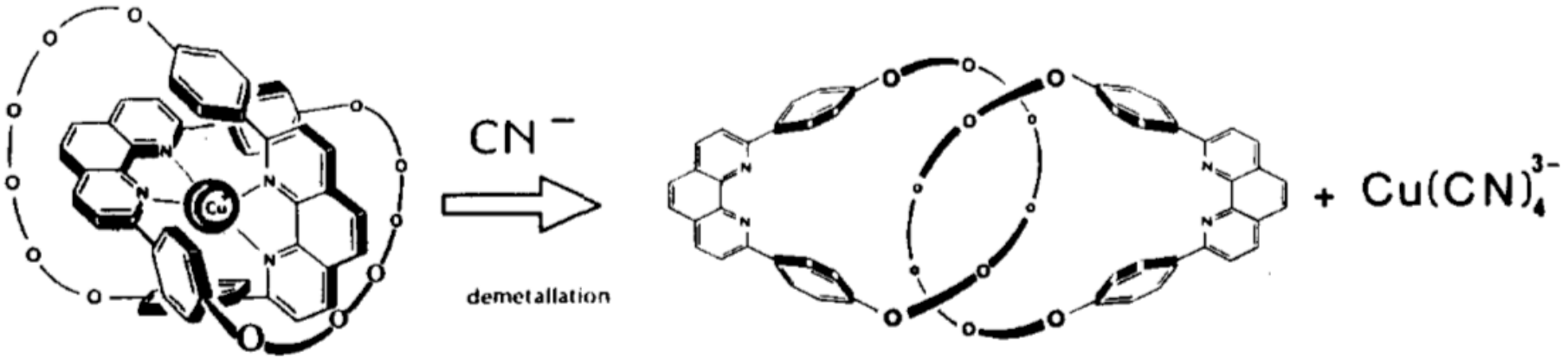

Dietrich-Buchecker, Sauvage, Kern, *J. Am. Chem. Soc.,* **1984,** 106, 3043.

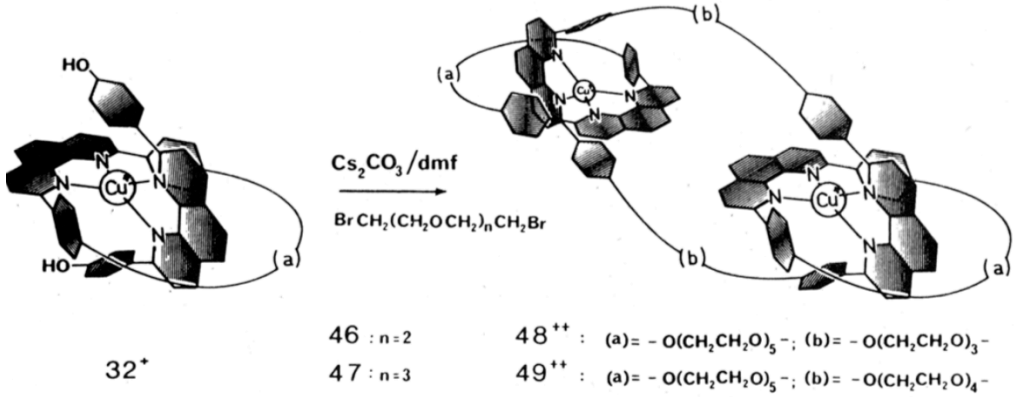

Sauvage, J. P.; Weiss, J. *J. Am. Chem.* Soc. **1985,** *107*, 6108.

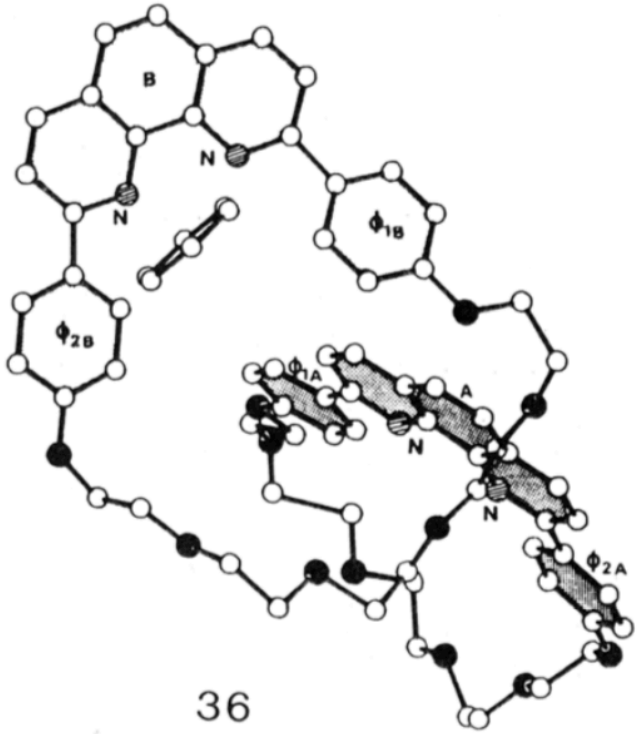

Catenanes: Molecular Knot

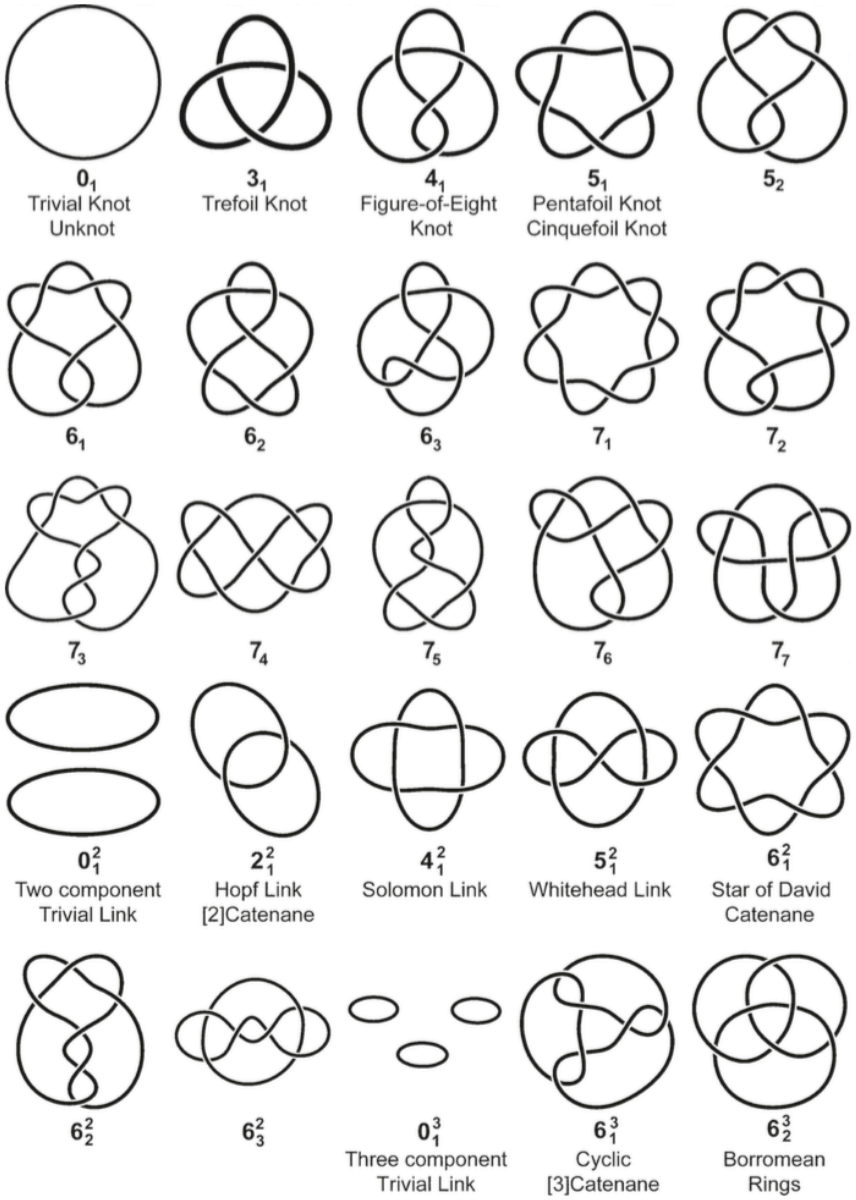

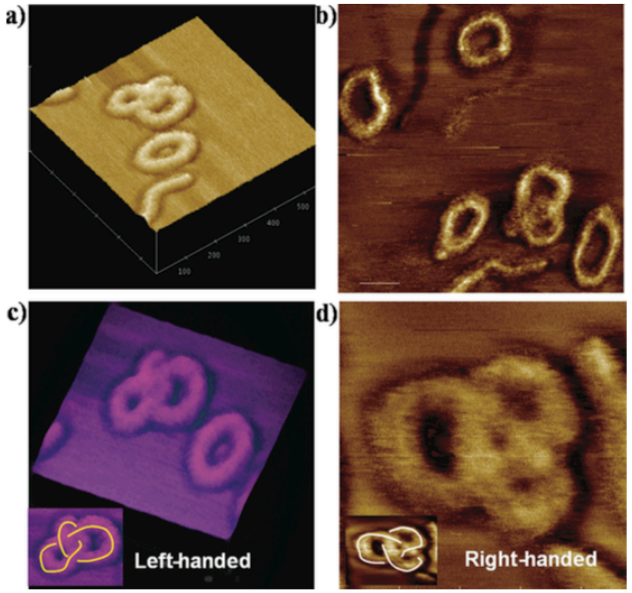

Figure 5. Topographic (a,c) and phase (b,d) AFM images of polymeric Trefoil Knots prepared by the cyclization of triblock copolymers. Note that images (c) and (d) are left- and right-handed versions of the Trefoil Knot, respectively. Reproduced with permission from ref 115. Copyright 2009 Wiley-VCH Verlag GmbH & Co. KGaA.

Catenanes: Molecular Knot

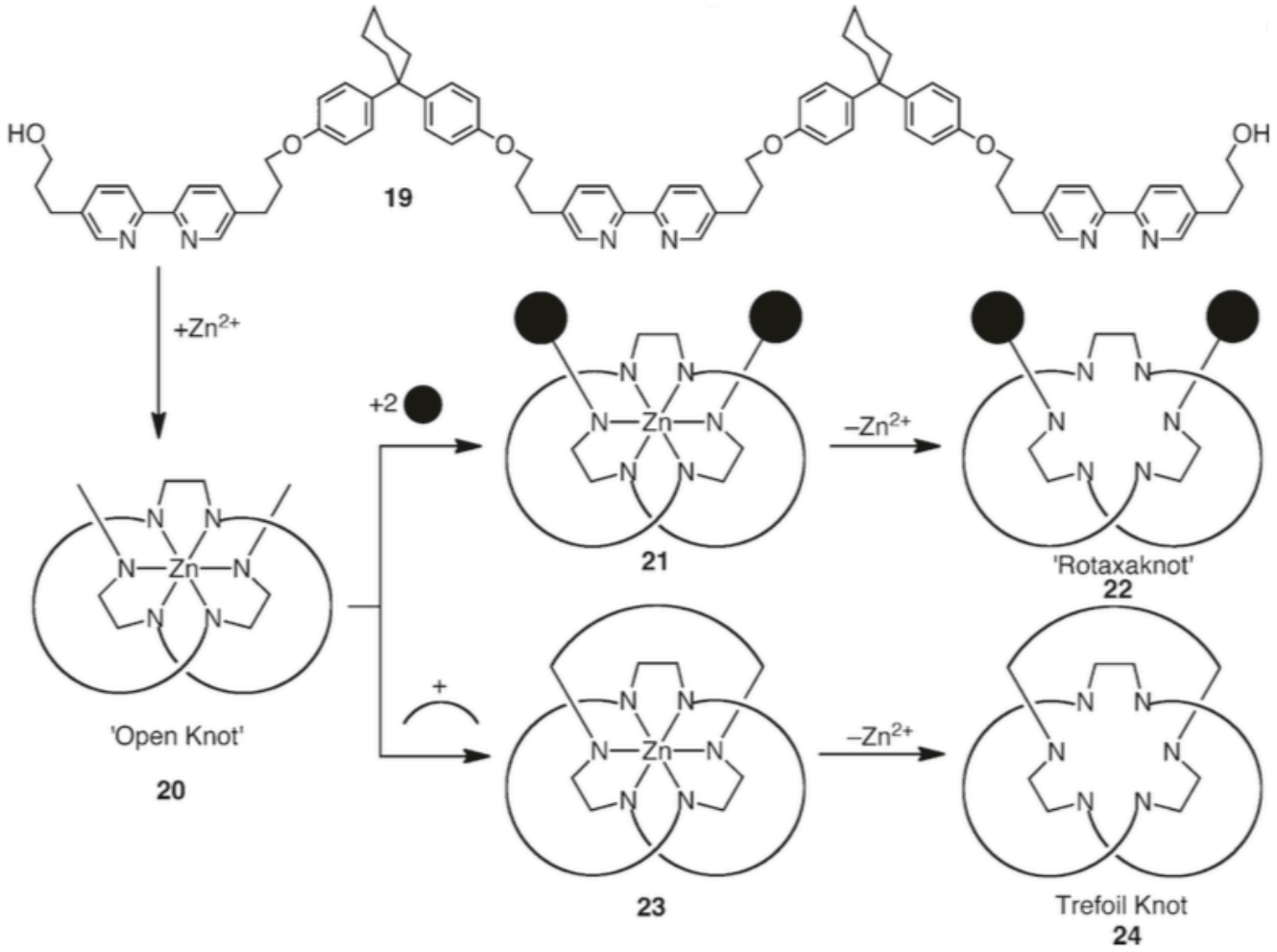

Adams, H.; Ashworth, E.; Breault, G. A.; Guo, J.; Hunter, C. A.; Mayers, P. C. *Nature* **2001**, 411, 763.
Guo, J.; Mayers, P. C.; Breault, G. A.; Hunter, C. A. *Nature Chem*. **2010**, 2, 218.

Catenanes: Molecular Knot

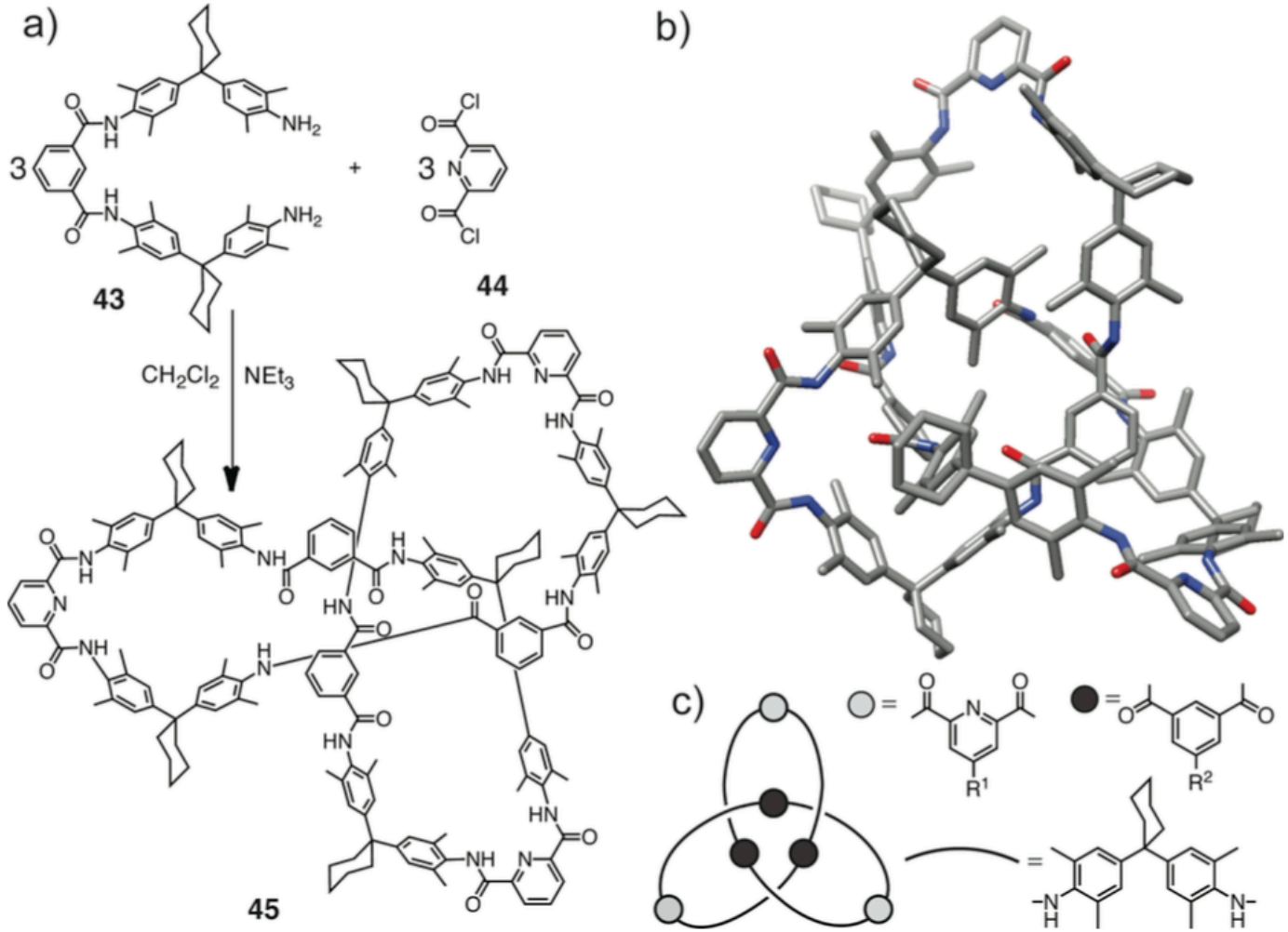

Safarowsky, O.; Nieger, M.; Frohlich, R.; Vogtle, F. *Angew. Chem., Int. Ed.* **2000,** *39*, 1616.

Catenanes: Molecular Knot

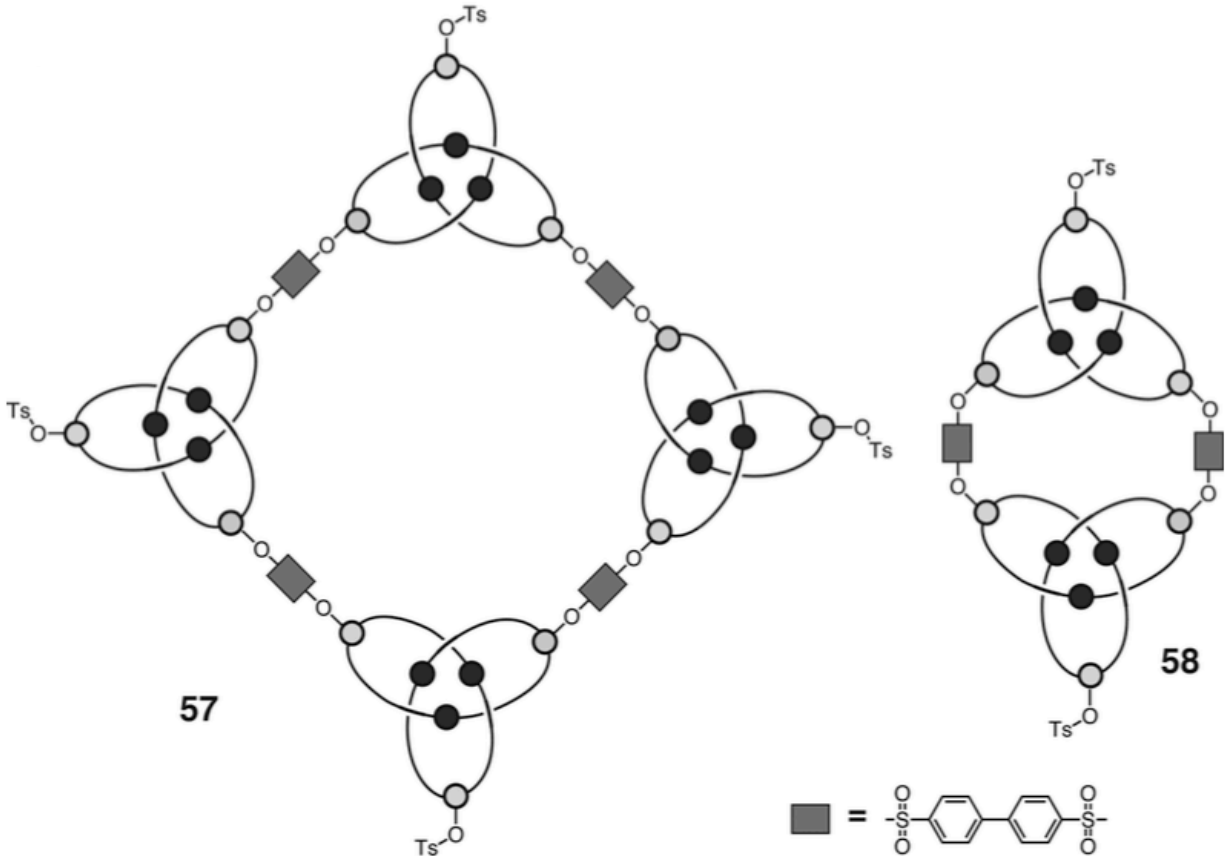

Lukin,O.;Kubota,T.;Okamoto,Y.;Kaufmann,A.;Vogtle,F. *Chem.-Eur. J.* **2004**, *10*, 2804.

Catenanes: Molecular Knot

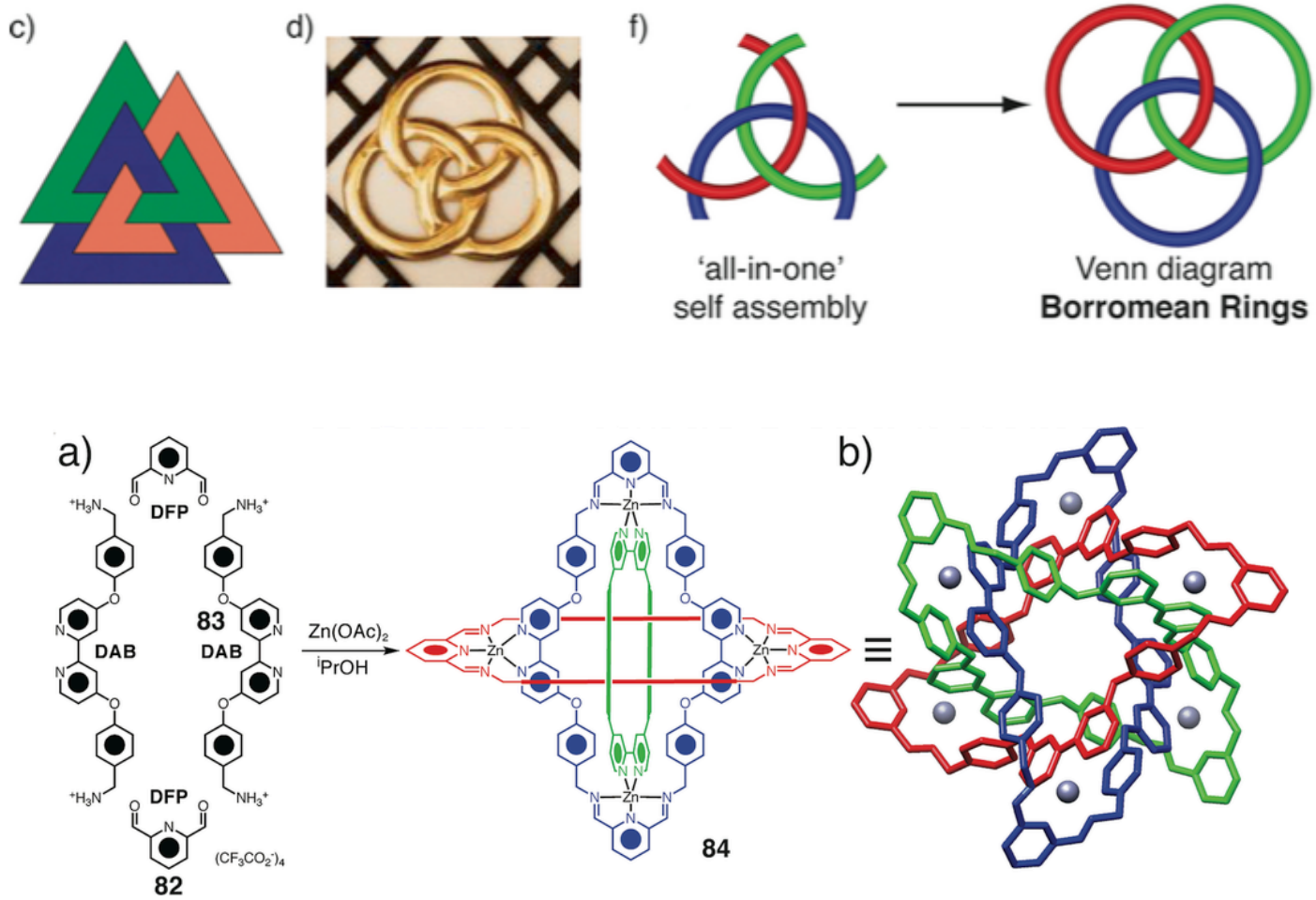

Figure 28. Molecular Borromean Rings.[300] (a) Schematic diagram to illustrate the synthesis in *i*PrOH of the Zn(II)-templated assembly **84** from $Zn(OAc)_2$, diformylpyridine (**DFP**, **82**), and the diaminobipyridine compound (**DAB**, **83**), which is generated in situ from its Boc-protected precursor (Boc-**DAB**) by deprotection with trifluoroacetic acid. (b) Tubular representation of the solid-state structure of **84** with each individual ring colored red, blue, and green and the Zn(II) cations depicted as silver spheres. Hydrogen atoms, solvents, and counterions are removed for clarity, generated from CCDC deposition 231701.

Chichak, K. S.; Cantrill, S. J.; Pease, A. R.; Chiu, S.-H.; Cave, G. W. V.; Atwood, J. L.; Stoddart, J. F. *Science* **2004**, 304, 1308

nature chemistry

ARTICLES

PUBLISHED ONLINE: 21 SEPTEMBER 2014 | DOI: 10.1038/NCHEM.2056

A Star of David catenane

David A. Leigh*, Robin G. Pritchard and Alexander J. Stephens

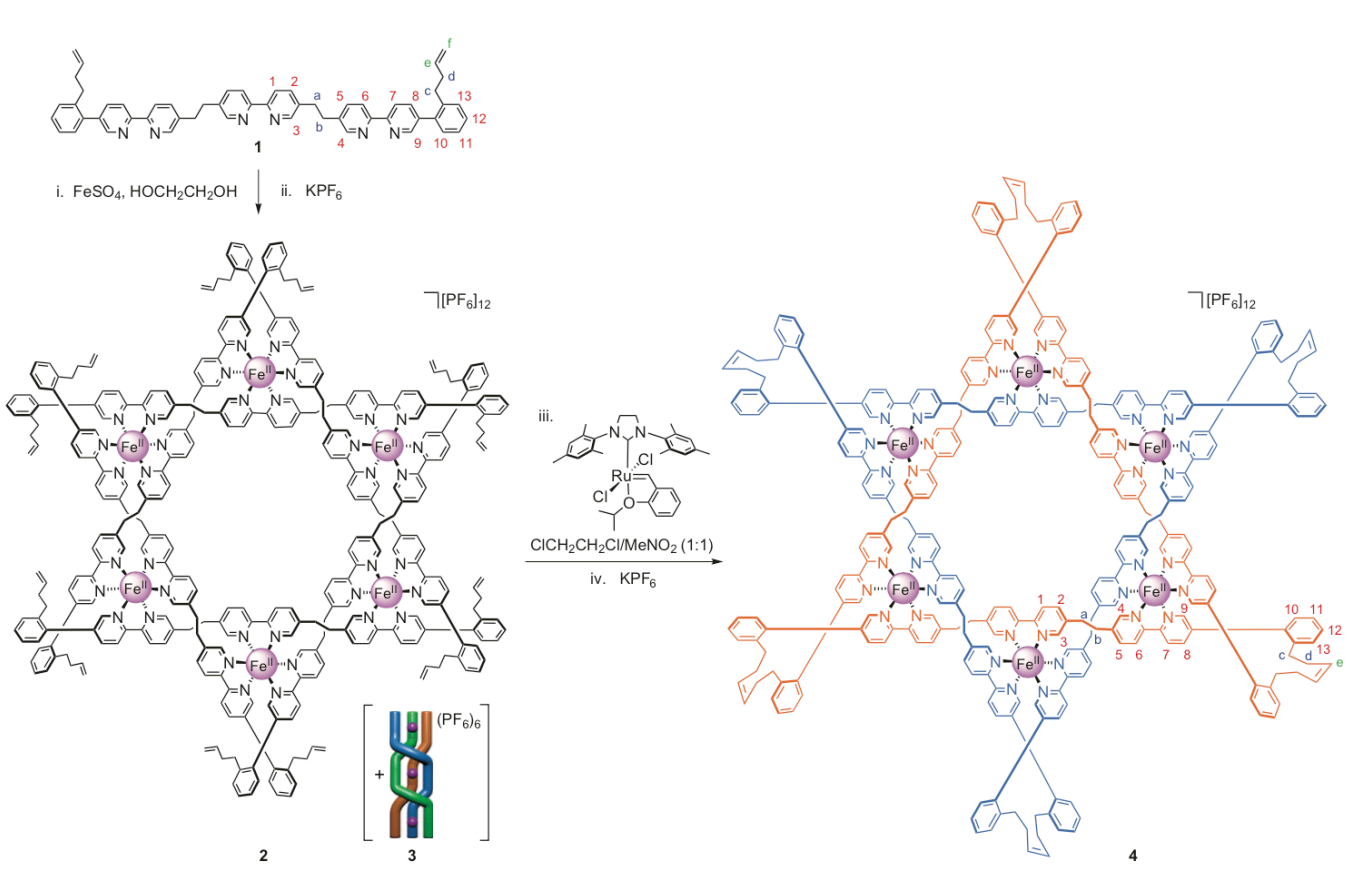

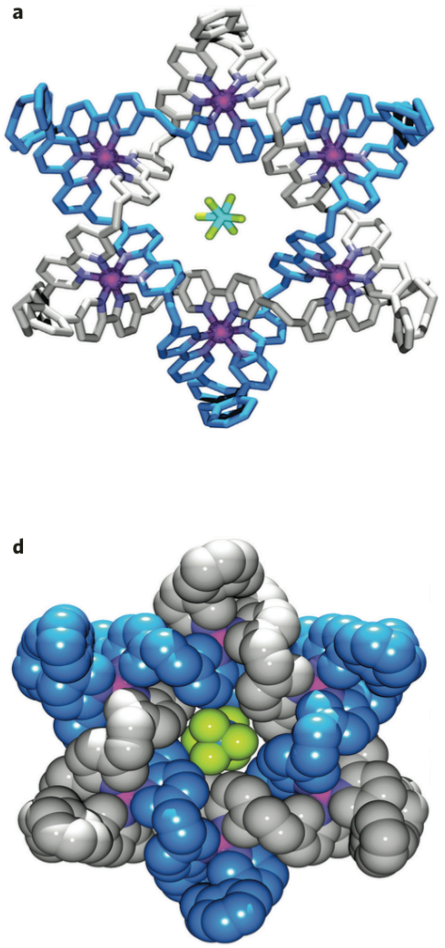

Figure 1 | Assembly of a hexameric circular iron(II) helicate [2](PF$_6$)$_{12}$ and subsequent ring closure to form a Star of David [2]catenate, [4](PF$_6$)$_{12}$. Reaction conditions: i, ethylene glycol, 170 °C, 24 hours; ii, excess saturated KPF_6 in methanol; iii, dichloroethane/nitromethane (1:1), 60 °C, 24 hours; iv, excess saturated aqueous KPF_6. The yields and ratios of circular double helicate [2](PF$_6$)$_{12}$ and linear triple helicate [3](PF$_6$)$_6$ vary with concentration and equivalents of $FeSO_4$ (see the Supplementary Information). In a representative procedure (14 mM **1**, 1 equiv. $FeSO_4$), [2](PF$_6$)$_{12}$ was isolated in 75% yield and [3](PF$_6$)$_6$ in 9% yield. Yield of [4](PF$_6$)$_{12}$ from [2](PF$_6$)$_{12}$, 92%.

Molecular Machines: Controlling movement

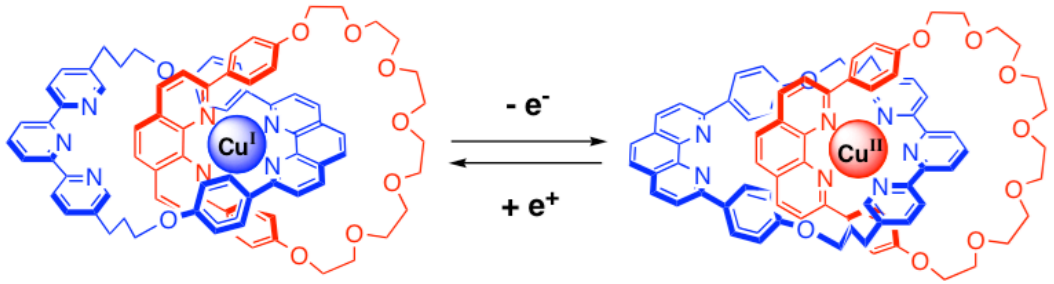

Livoreil, A.; Dietrich-Buchecker, C. O.; Sauvage, J.-P.
J. Am. Chem. Soc. **1994**, *116*, 9399-9400.

Pirouetting-Controlled Rotaxane Switch

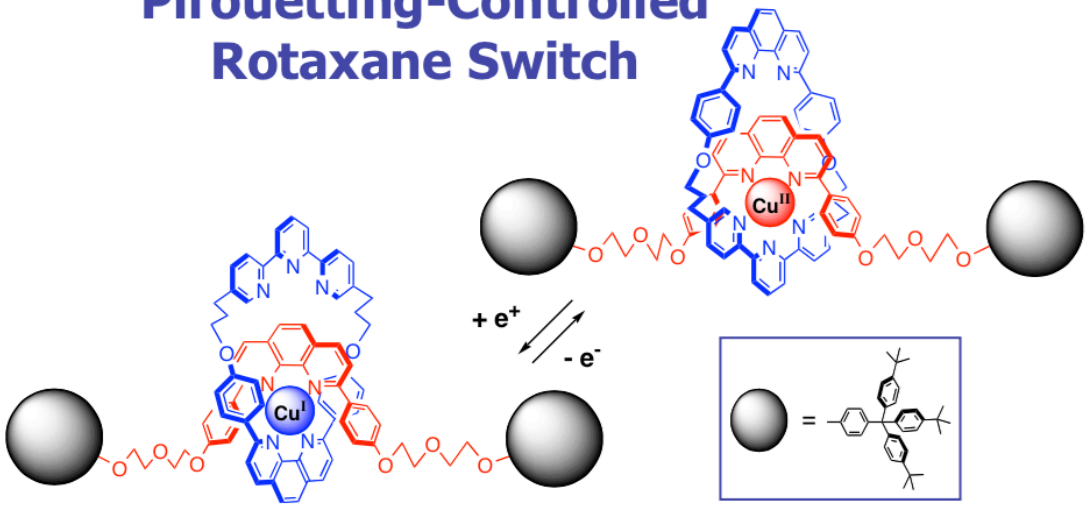

Kern, J.-M.; Raehm, L.; Sauvage, J.-P.; Divisia-Blohorn, B.; Vidal, P.-L.
Inorg. Chem. **2000**, *39*, 1555-1560.

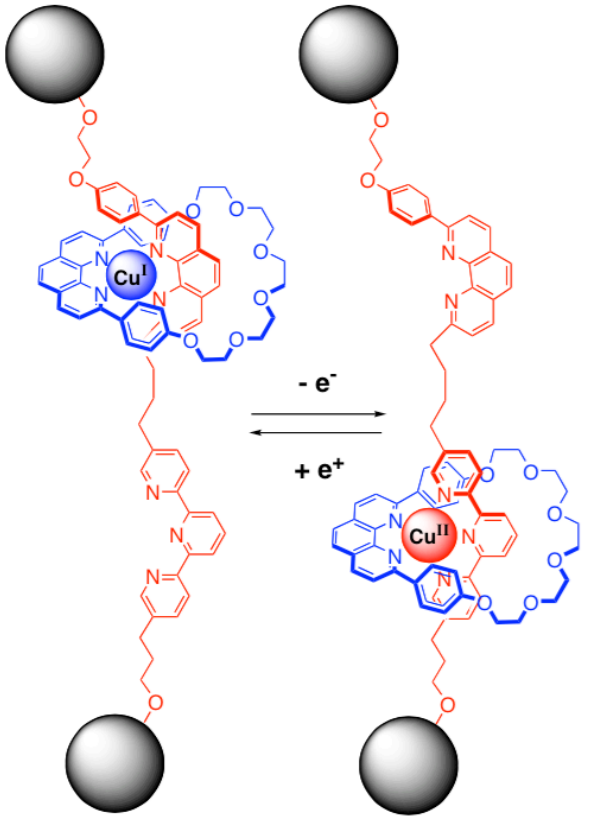

Armaroli, N.; Balzani, V.; Collin, J.-P.; Gavin, P.; Sauvage, J.-P.; Ventura, B. *J. Am. Chem. Soc.* **1999**, *121*, 4397-4408.

Molecular Machines: Examples

Propeller

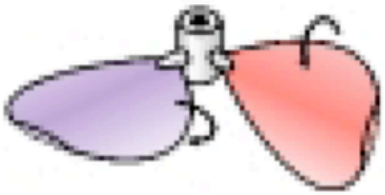

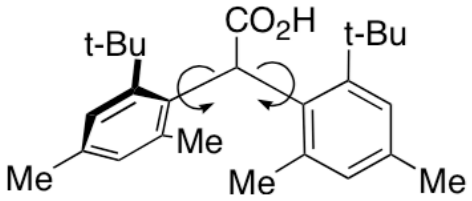

Akkerman, O. S.; Coops, J. *Rec. Trav. Chim. Pays-Bas* **1967**, *86*, 755-761; *ibid.* **1970**, *89*, 673-679.

Turnstile

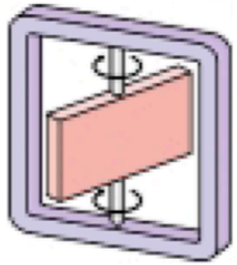

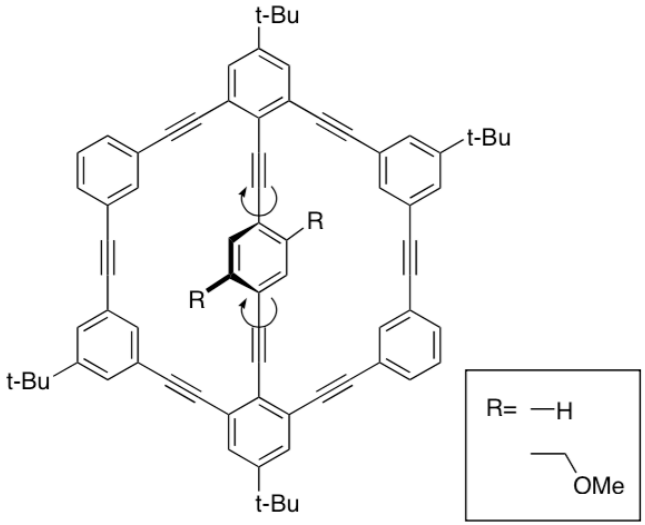

Bedard, T. C.; Moore, J. S. *J. Am. Chem. Soc.* **1995**, *117*, 10662-10671.

Gear

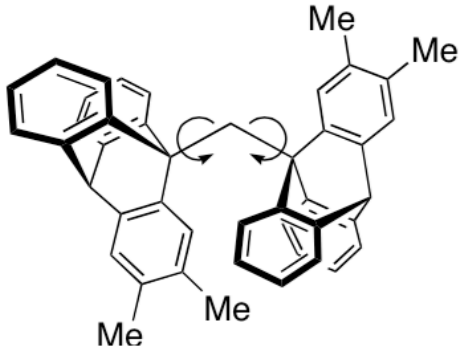

Cozzi, F.; Guenzi, A.; Johnson, C. A.; Mislow, K.; Hounshell, W. D.; Blount, J. F. *J. Am. Chem. Soc.* **1981**, *103*, 957-958.

Molecular Machines: Controlling rotation

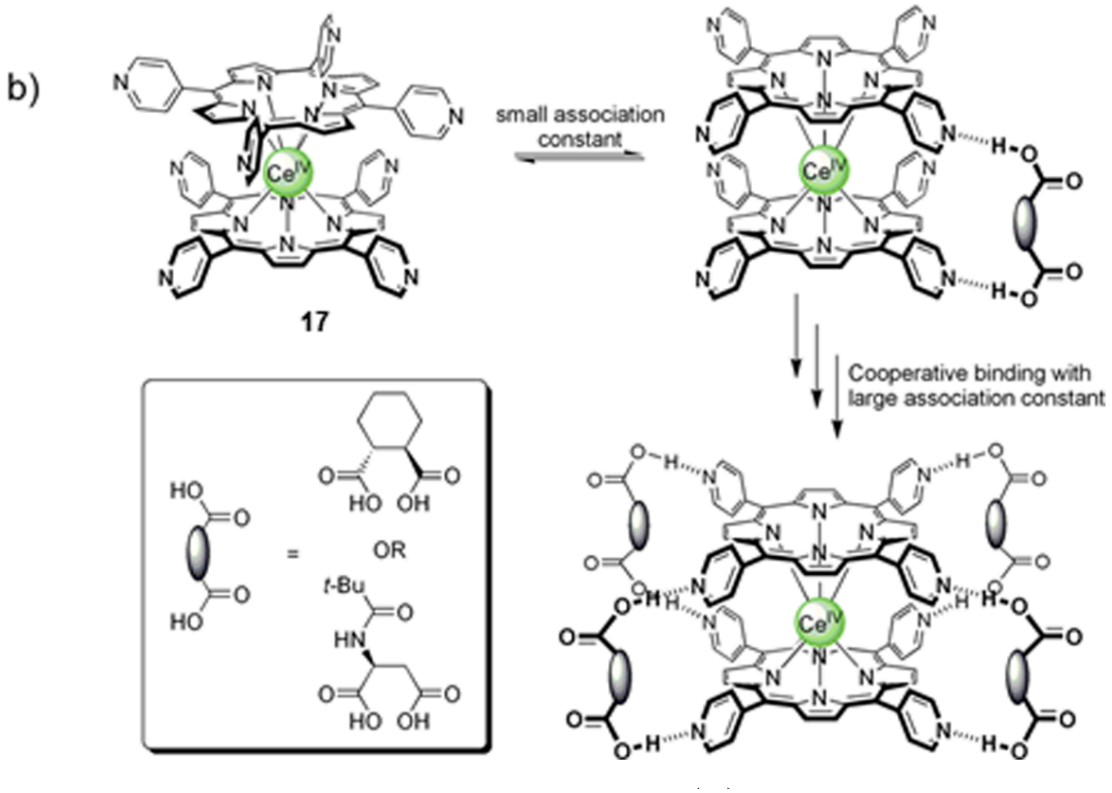

Takeuchi, M.; Imada, I.; Shinkai, S, *Angew. Chem., Int. Ed.* **1998**, 37, 2096

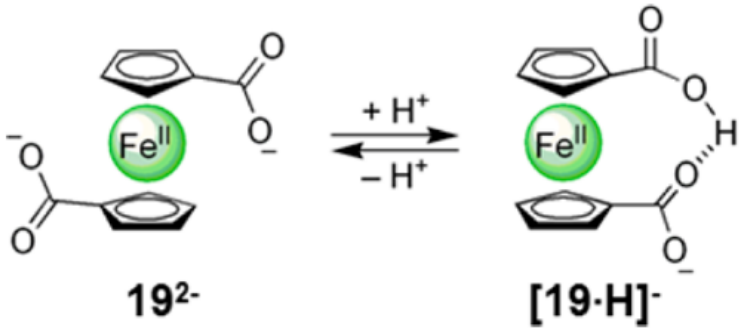

Wang, X. B.; Dai, B.; Woo, H. K.; Wang, L. S. *Angew. Chem., Int. Ed.* **2005**, 44, 6022

Molecular Machines: Controlling movement

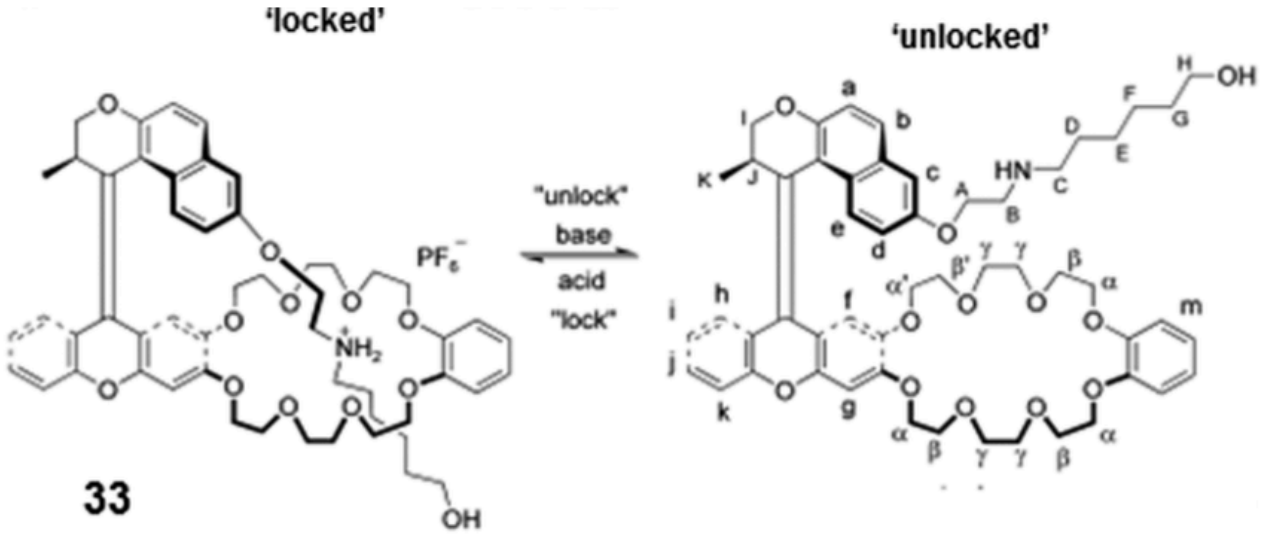

Qu, D.-H.; Feringa, B. L. *Angew. Chem., Int. Ed.* **2010**, *49*, 1107− 1110.

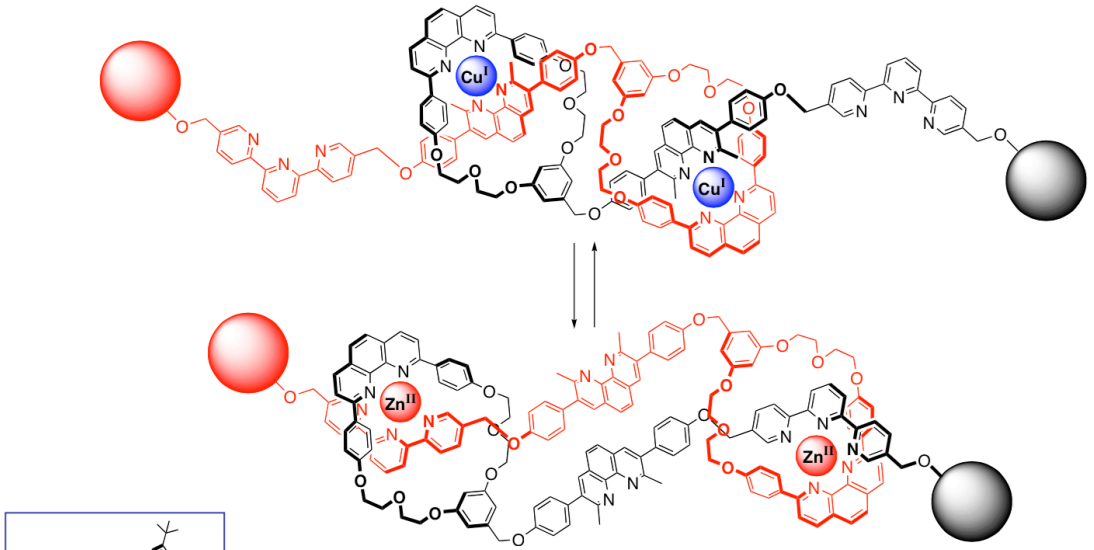

Jimenez, M. C.; Dietrich-Buchecker, C.; Sauvage, J.-P. *Angew. Chem. Int. Ed.* **2000**, *39*, 3284-3287.
Jimenez-Molero, M. C.; Dietrich-Buchecker, C.; Sauvage, J.-P. *Chem. Commun.* **2003**, 1613-1616.

Molecular Machines: Controlling movement, a molecular crank

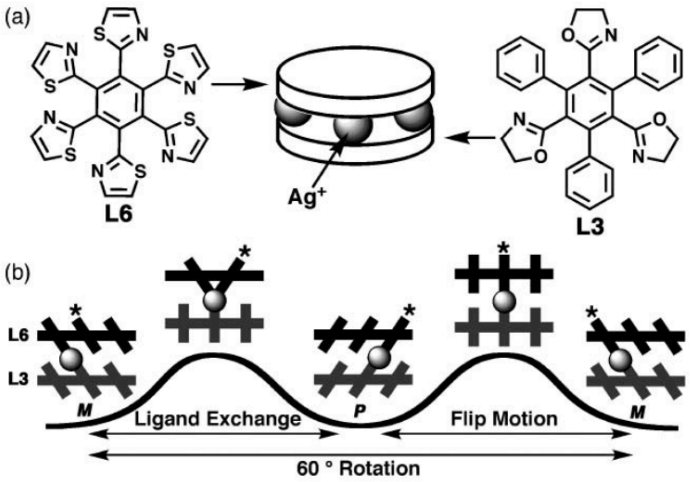

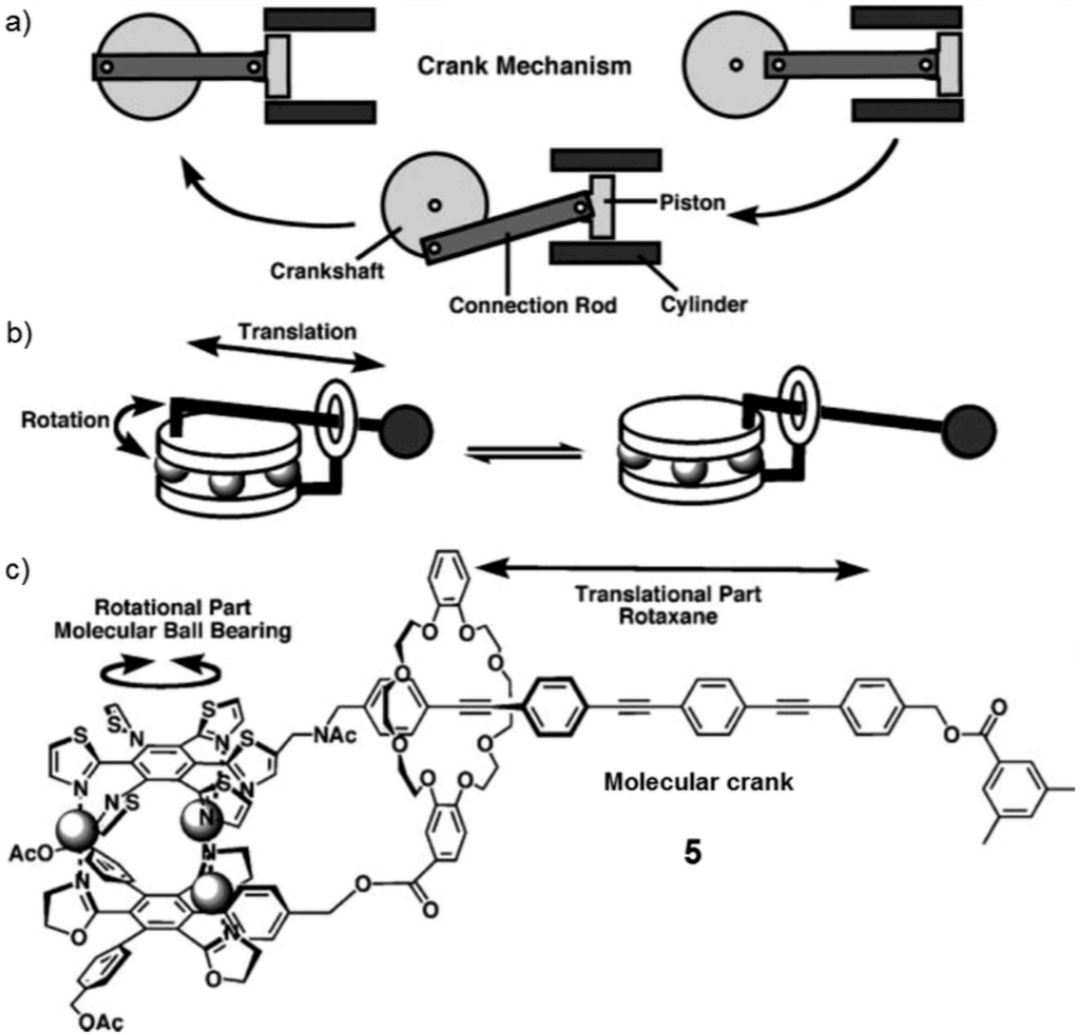

Okuno, E.; Hiraoka, S.; Shionoya, M. A, *Dalton Trans*. **2010**, 39, 4107−4116.

Molecular Machines: Molecular Gate

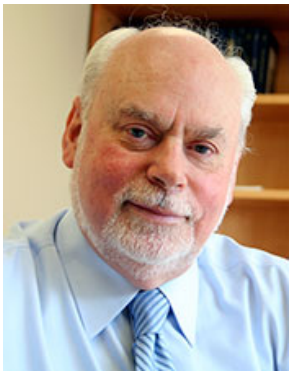

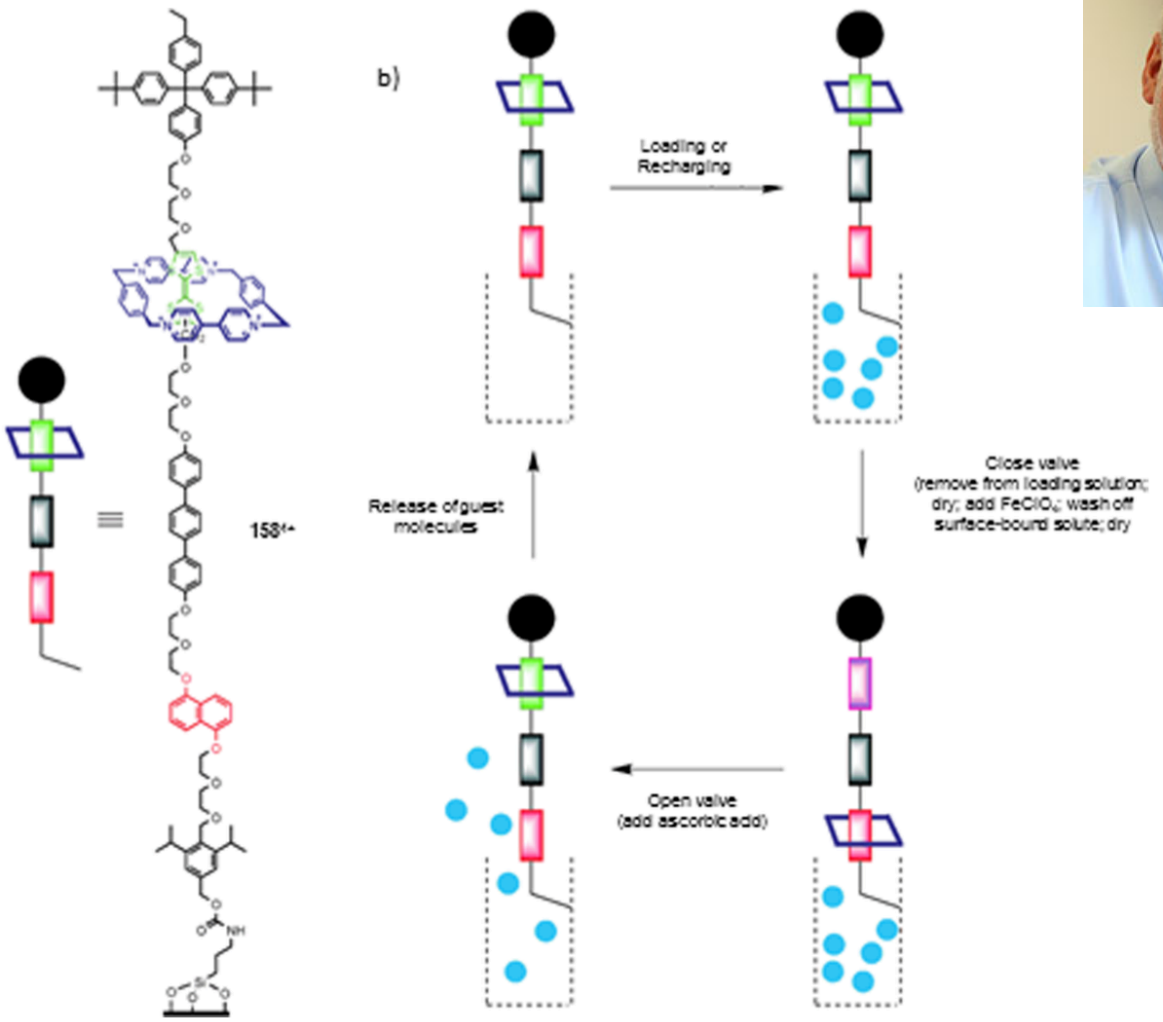

Nguyen, T. D.; Tseng, H.-R.; Celestre, P. C.; Flood, A. H.; Liu, Y.; Stoddart, J. F.; Zink, J. I. *Proc. Natl. Acad. Sci. U. S. A*. **2005**, 102, 10029

Molecular Machines: A Molecular Elevator

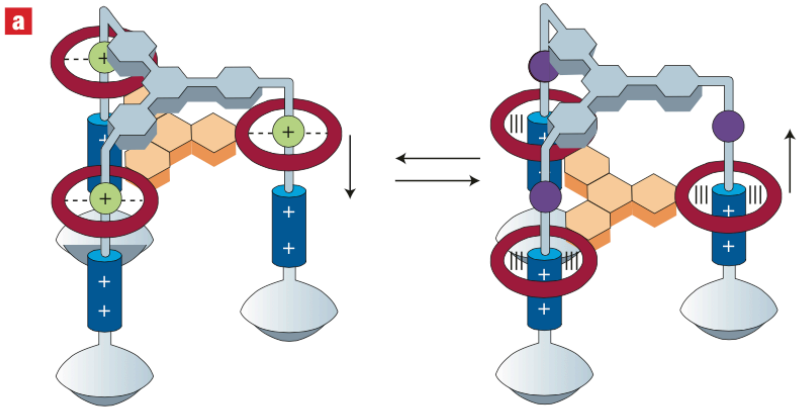

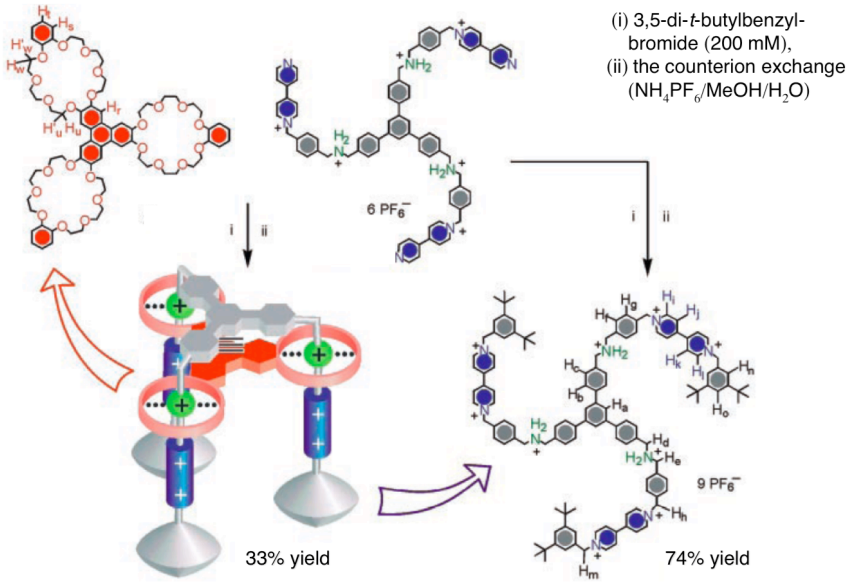

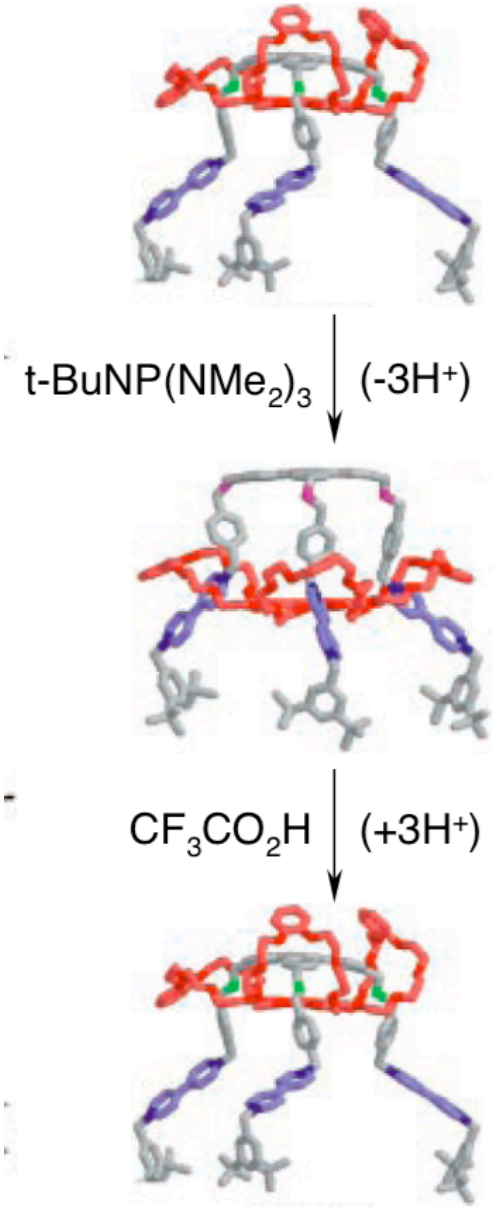

Badjic, J. D.; Balzani, V.; Credi, A.; Silvi, S.; Stoddart, J. F., *Science* **2004**, 303, 1845.

Stoddart. *J. Am. Chem. Soc.*, **2006** 128, 1489

Molecular Machines: Molecular Valves

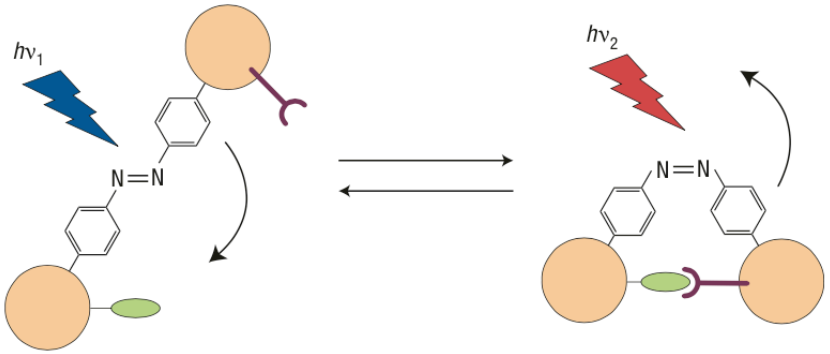

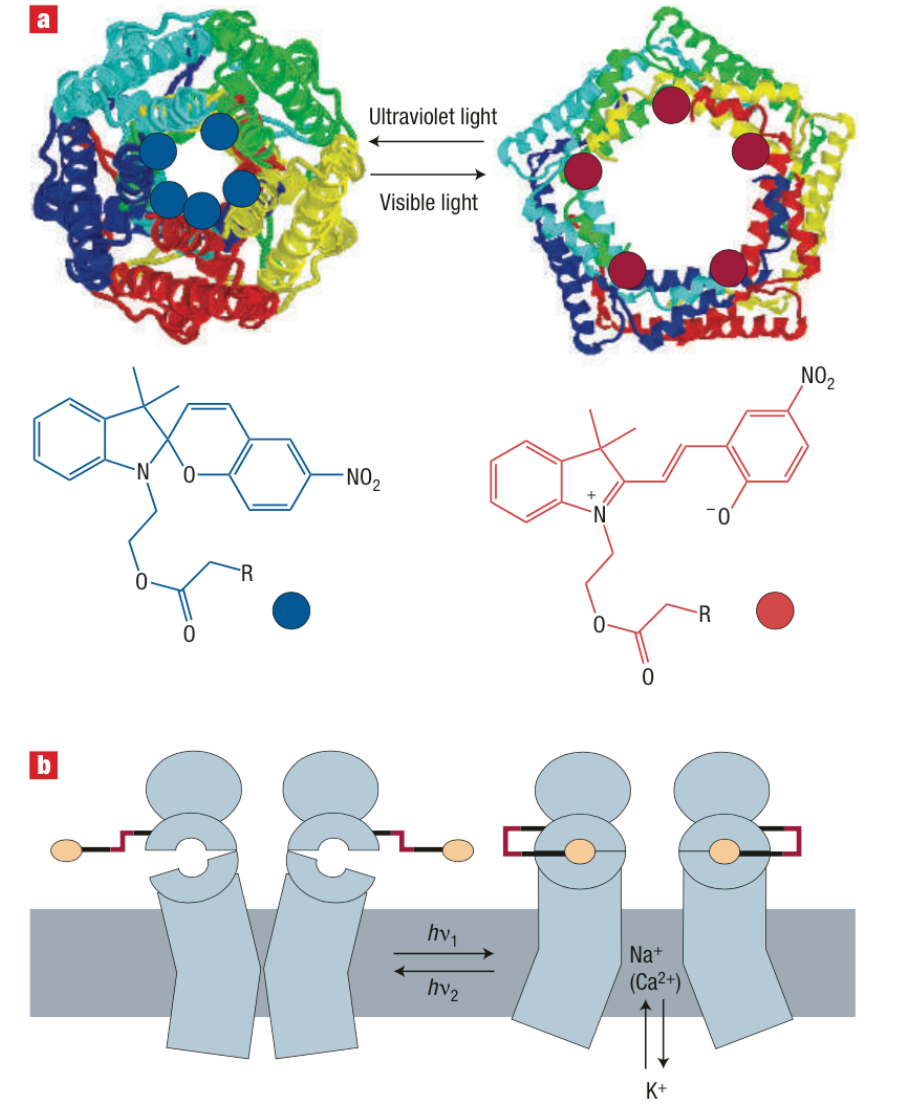

A light-actuated nanovalve based on a mechanosensitive channel protein modified with spiropyran photoswitches. When ultraviolet light is shone on the protein, the molecular switch is converted from its neutral, hydrophobic, form to a charged polar form. The change in hydrophobicity in the channel results in the channel opening. Visible light reverses the process and closes the channel again.

B. Photochemical allosteric control of a glutamate- sensitive protein channel based on the azobenzene molecular switch. In this example, the switching unit is not incorporated in the channel itself but instead is located on the outside of the channel protein. When light is shone on the azobenzene switch, the glutamate is brought into contact with a receptor site on the outside of the protein. The binding of glutamate to this site results in opening of the protein valve. Again, the process is reversed by shining light of a different colour on the protein, which moves the glutamate away from the control site.

Koçer, A., Walko, M., Meijberg, W. & Feringa B. L. *Science*, **2005**, 309, 75
Volgraf, M. et al. *Nature Chem. Biol.* **2006**, 2, 47

Molecular Machines: Triggering Catalysts

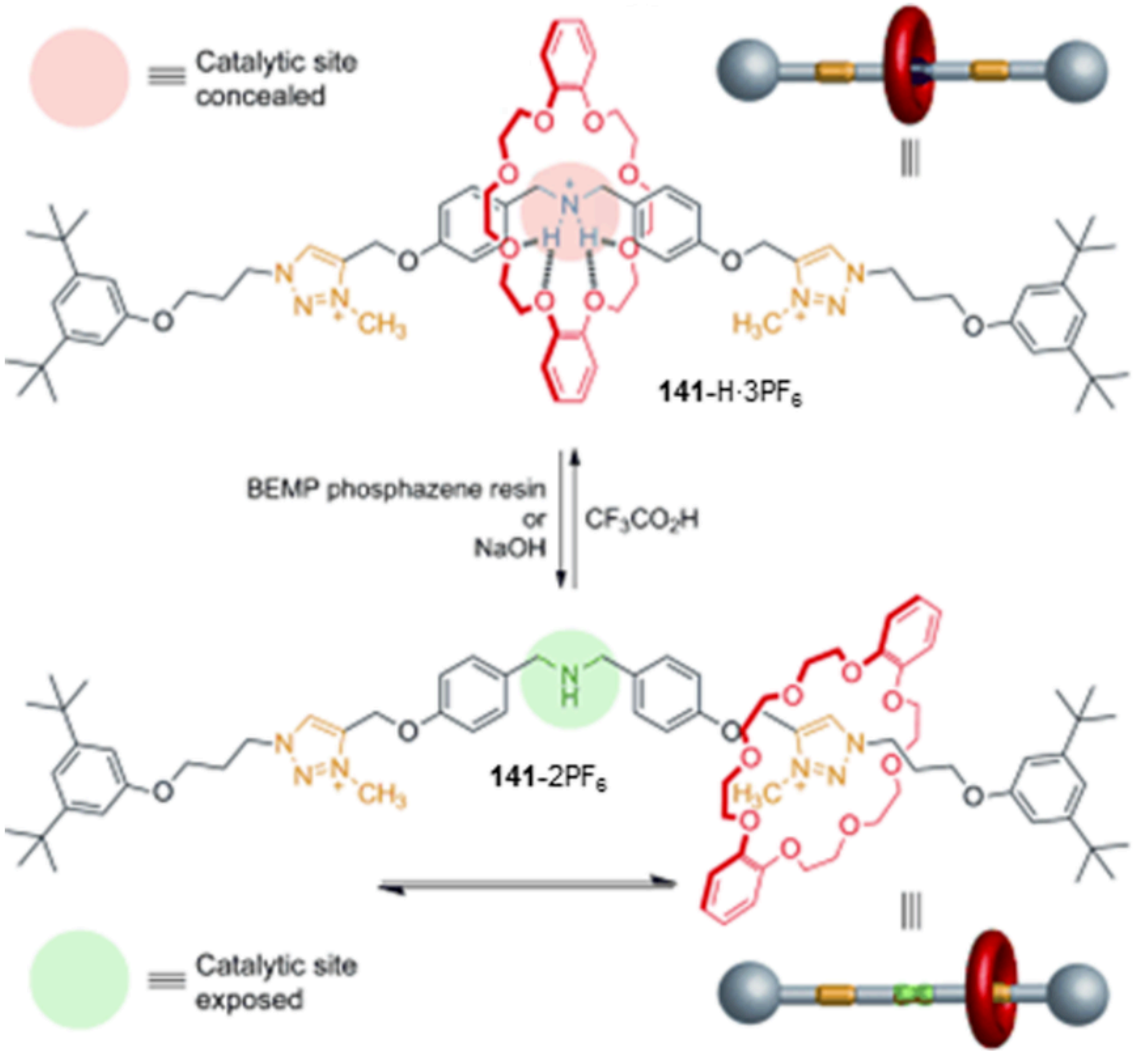

Blanco, V.; Carlone, A.; Hanni, K. D.; Leigh, D. A.; Lewandowski, B.
Angew. Chem., Int. Ed. **2012**, 51, 5166

ARTICLES
PUBLISHED ONLINE: 20 DECEMBER 2009 | DOI: 10.1038/NCHEM.481
nature chemistry

A synthetic small molecule that can walk down a track

Max von Delius, Edzard M. Geertsema and David A. Leigh*

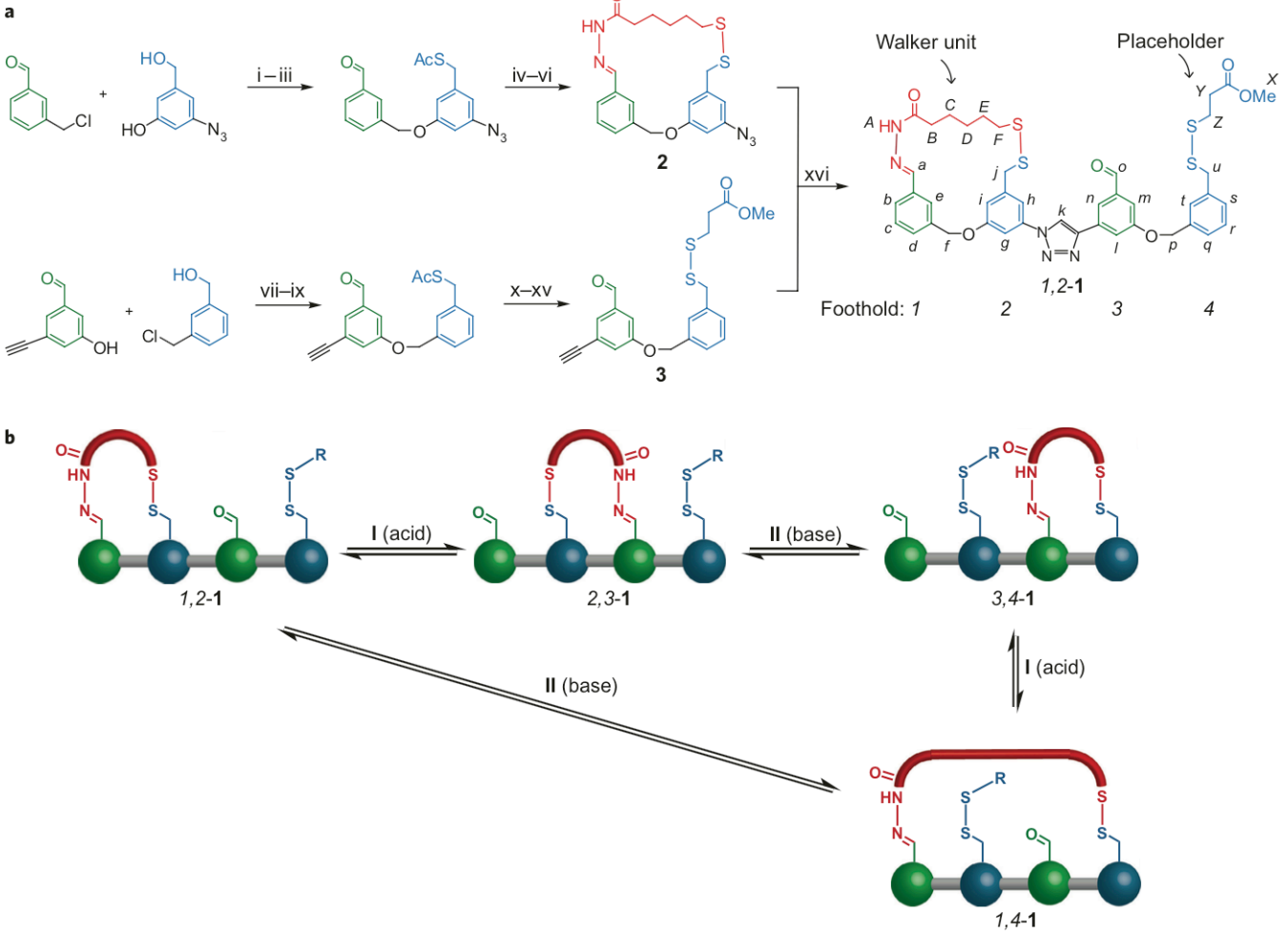

Macroscopic transport by synthetic molecular machines

JOSÉ BERNÁ[1], DAVID A. LEIGH[1]*, MONIKA LUBOMSKA[2], SANDRA M. MENDOZA[2], EMILIO M. PÉREZ[1], PETRA RUDOLF[2]*, GILBERTO TEOBALDI[3] AND FRANCESCO ZERBETTO[3]*

[1]School of Chemistry, University of Edinburgh, The King's Buildings, West Mains Road, Edinburgh EH9 3JJ, UK
[2]Materials Science Centre, Rijksuniversiteit Groningen, Nijenborgh 4, 9747AG Groningen, The Netherlands
[3]Dipartimento di Chimica 'G. Ciamician', Università degli Studi di Bologna, v. F. Selmi 2, 40126 Bologna, Italy
*e-mail: David.Leigh@ed.ac.uk; P.Rudolf@rug.nl; francesco.zerbetto@unibo.it

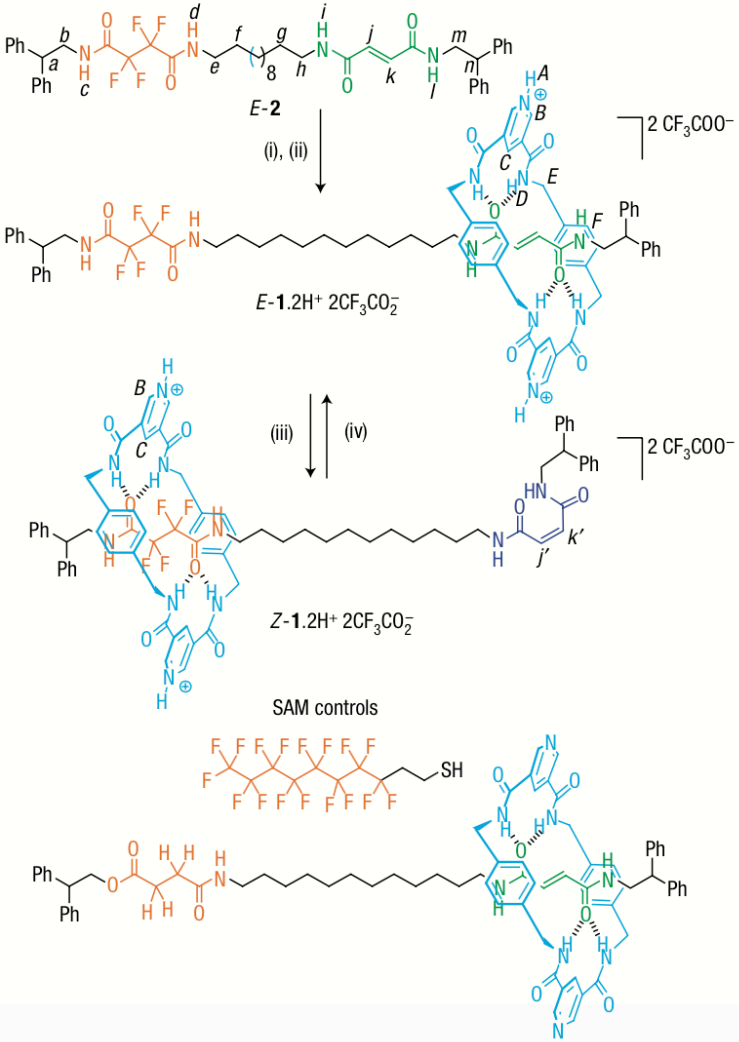

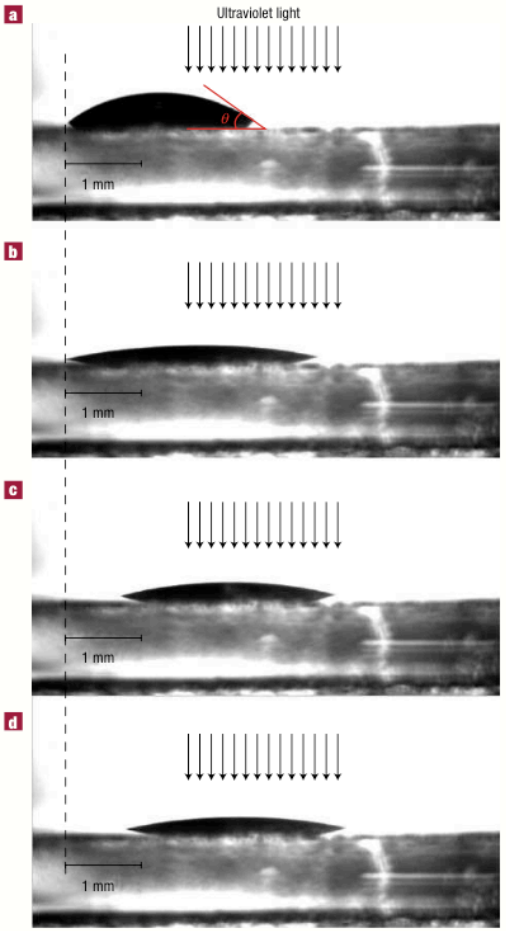

Figure 5 Lateral photographs of light-driven directional transport of a 1.25 μl diiodomethane drop across the surface of a *E*-1.11-MUA.Au(111) substrate on glass. The direction of transportation was controlled by irradiation with a perpendicular beam of 240–400 nm light focused on one side of the drop and the adjacent surface. The irradiation time required for transport and the distance the droplet travels depends on the precise position of the lamp. **a**, Before irradiation

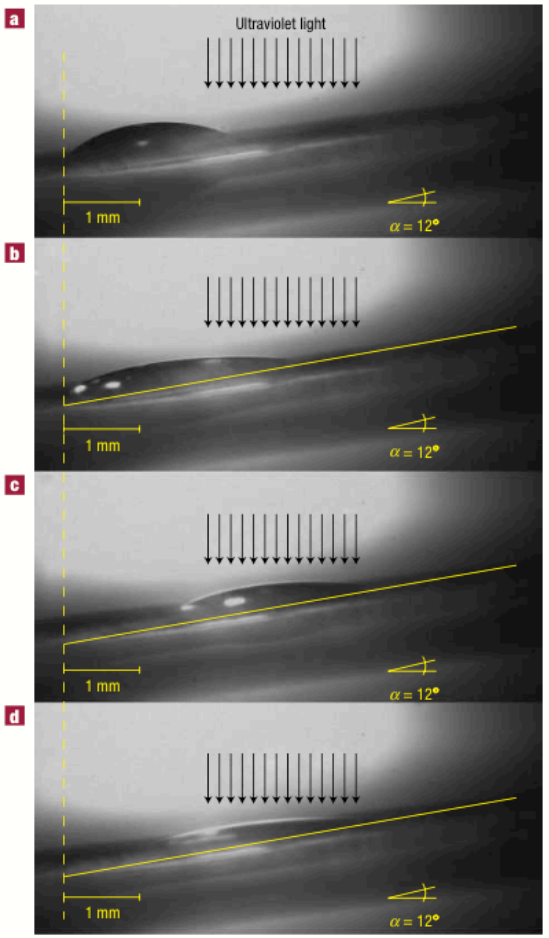

Figure 7 Lateral photographs of light-driven transport of a 1.25 μl diiodomethane drop on a *E*-1.11-MUA.Au(111) substrate on mica up a 12° incline. For clarity, on photographs **b**–**d** a yellow line is used to indicate the surface of the substrate. **a**, Before irradiation (pristine *E*-**1**). **b**, After 160 s of irradiation (just

Unidirectional rotation in a mechanically interlocked molecular rotor

David A. Leigh*, Jenny K. Y. Wong*, François Dehez† & Francesco Zerbetto†

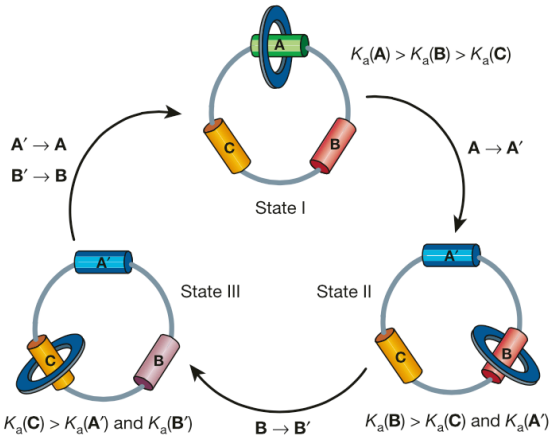

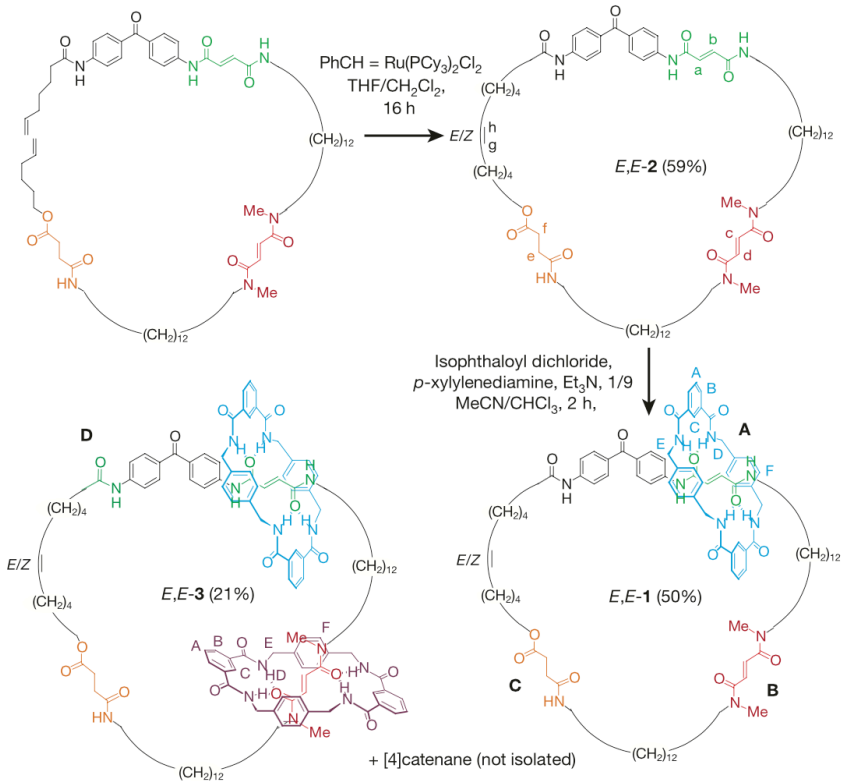

Figure 2 Ring-closing reactions to form macrocycle *E,E*-**2**, [2]catenane *E,E*-**1** and [3]catenane *E,E*-**3**. Closure of the large macrocycle, *E,E*-**2**, proceeds via ring-closing metathesis with the first-generation Grubbs catalyst PhCH = $Ru(PCy_3)_2Cl_2$ (ref. 19). The remarkable yield (59%) for the formation of the 63-membered ring is probably a result of intramolecular hydrogen bonding folding the open-chain precursor. The coloured letters indicate ^{1}H assignments in Figs 3B and 4.

Unidirectional rotation in a mechanically interlocked molecular rotor

David A. Leigh*, Jenny K. Y. Wong*, François Dehez† & Francesco Zerbetto†

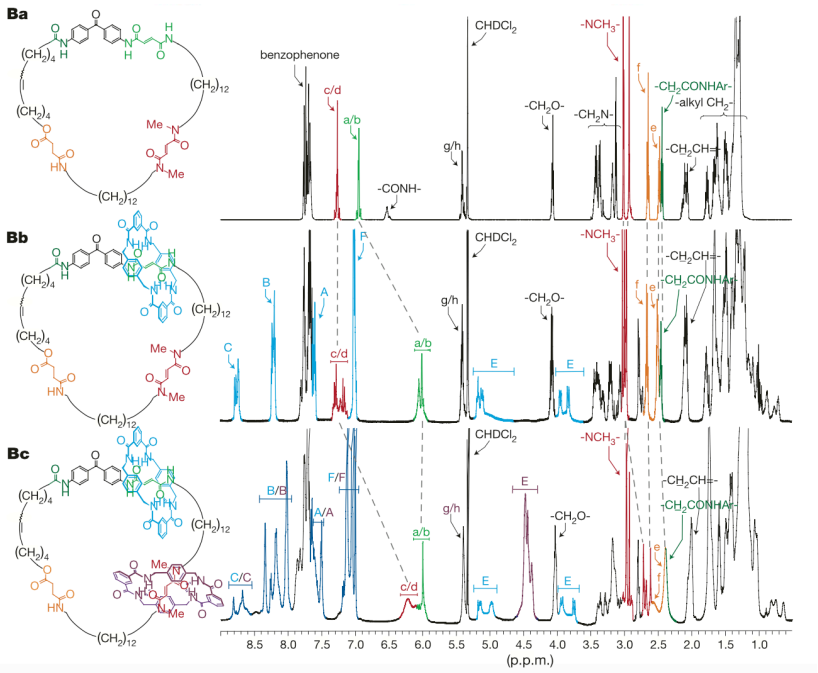

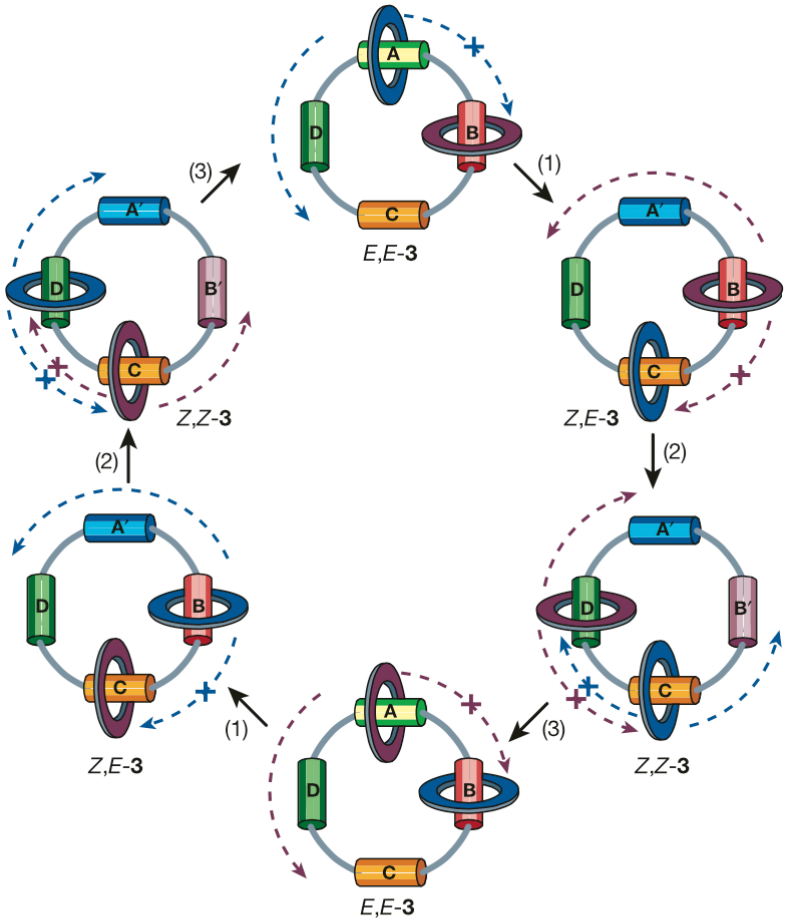

Figure 5 Stimuli-induced unidirectional rotation in a four-station [3]catenane, **3**. (1) 350 nm, CH_2Cl_2, 5 min, 67%; (2) 254 nm, CH_2Cl_2, 20 min, 50%; (3) heat, 100 °C, $C_2H_2Cl_4$, 24 h, ~100%; catalytic ethylenediamine, 50 °C, 48 h, 65%; or catalytic Br_2, 400–670 nm, CH_2Cl_2, −78 °C, 10 min, ~100%.

A molecular information ratchet

Viviana Serreli[1], Chin-Fa Lee[1], Euan R. Kay[1] & David A. Leigh[1]

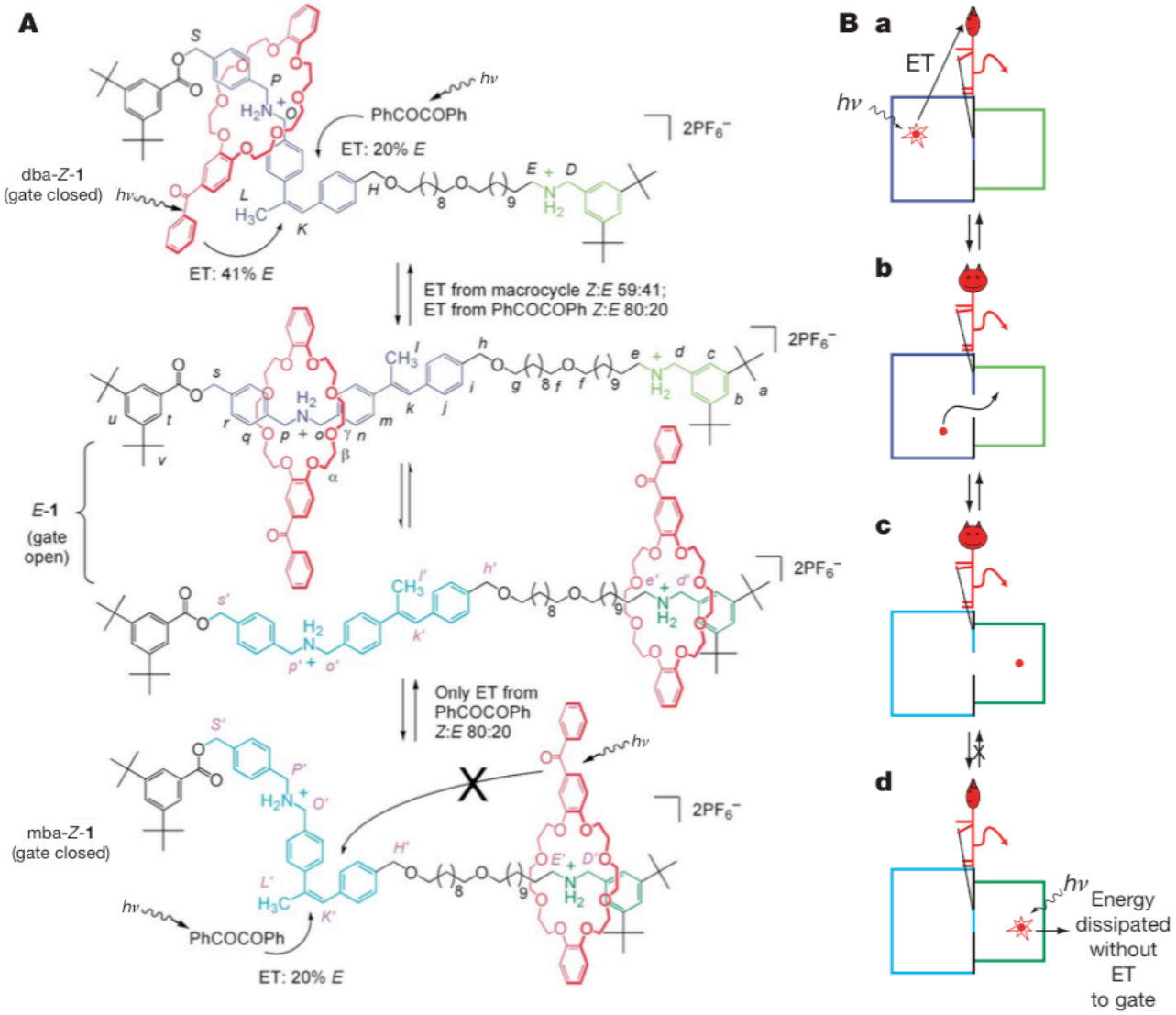

Molecular Machines: Toward Artificial Muscles

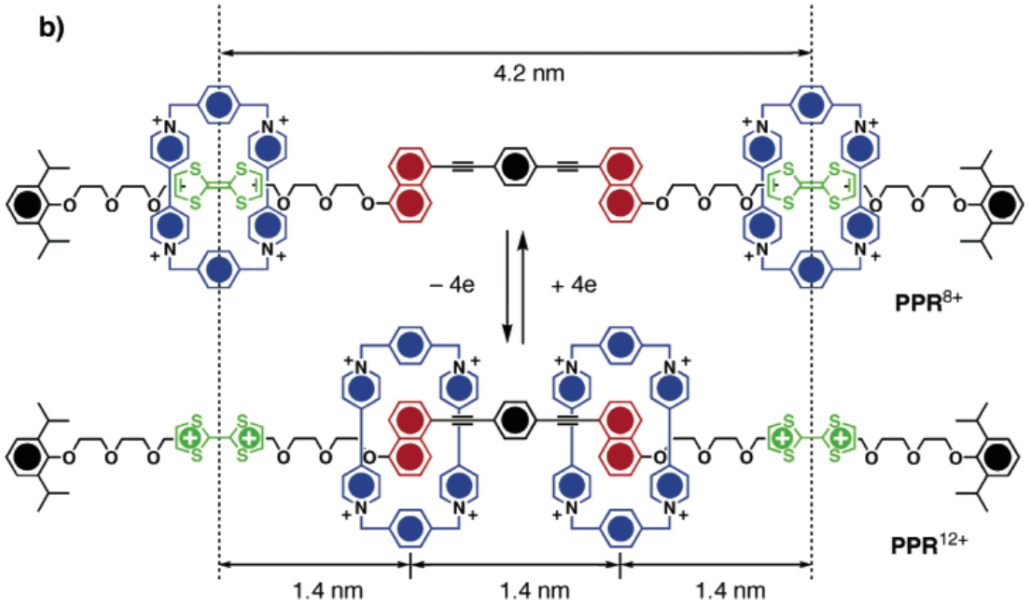

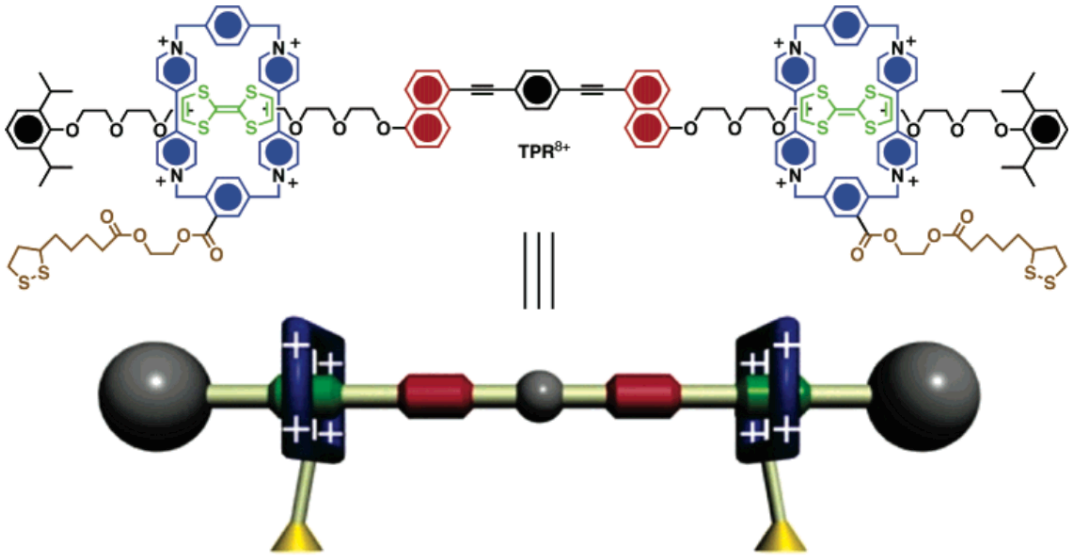

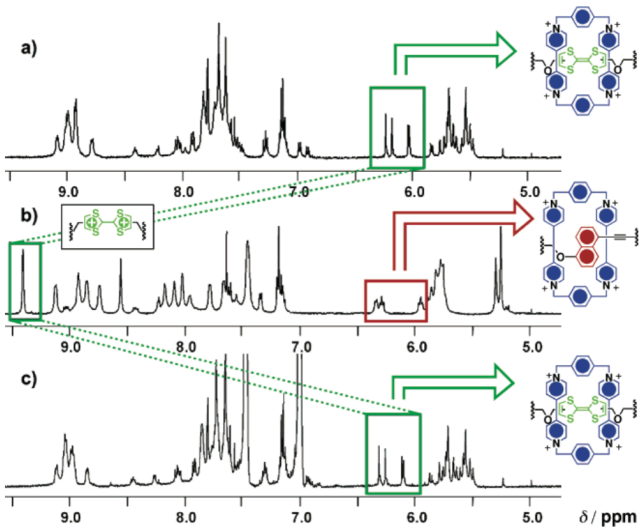

Stoddart, *J. Am. Chem. Soc.*, **2005**, *127*, 9745

Molecular Machines: Toward Artificial Muscles

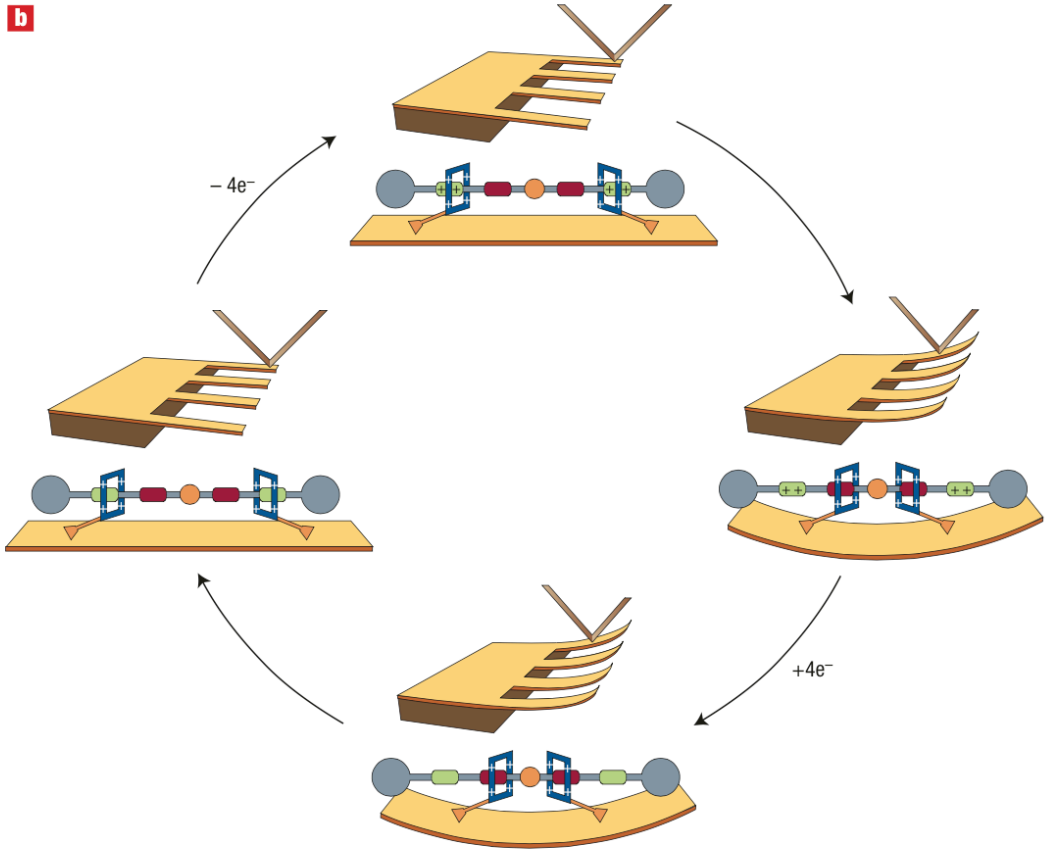

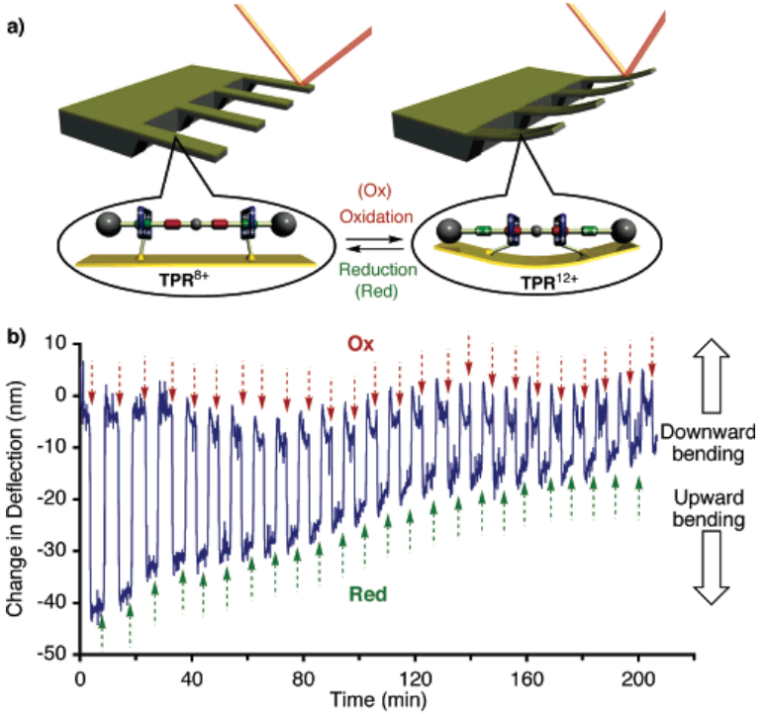

Berna, J. et al. *Nature Mater*. **2005**, 4, 704

Stoddart, *J. Am. Chem. Soc.*, **2005**, *127*, 9745